PL-TR-97-2077

DEVELOPMENT OF DISCRIMINATION, DETECTION, AND LOCATION CAPABILITIES IN CENTRAL AND SOUTHERN ASIA USING MIDDLE-PERIOD SURFACE WAVES RECORDED BY A REGIONAL ARRAY

Anatoli L. Levshin
Michael H. Ritzwoller

University of Colorado
Department of Physics
Campus Box 583
Boulder, CO 80309-0583

10 June 1997

Final Report
15 June 1995 -14 June 1997

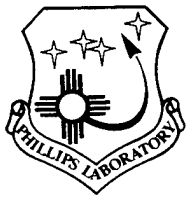

PHILLIPS LABORATORY
Directorate of Geophysics
AIR FORCE MATERIEL COMMAND
HANSCOM AFB, MA 01731-3010

SPONSORED BY
Air Force Technical Applications Center
Directorate of Nuclear Treaty Monitoring
Project Authorization T/5101

MONITORED BY
Phillips Laboratory
CONTRACT No. F19628-95-C-0099

The views and conclusions contained in this document are those of the authors and should not be interpreted as representing the official policies, either express or implied, of the Air Force or U.S. Government.

This technical report has been reviewed and is approved for publication.

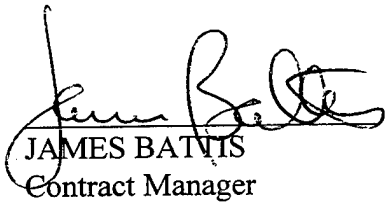

JAMES BATTIS
Contract Manager
Space Effects Division

DAVID A. HARDY
Director
Space Effects Division

This report has been reviewed by the ESD Public Affairs Office (PA) and is releasable to the National Technical Information Service (NTIS).

Qualified requestors may obtain copies from the Defense Technical Information Center. All others should apply to the National Technical Information Service.

If your address has changed, or you wish to be removed from the mailing list, or if the addressee is no longer employed by your organization, please notify PL/IM, 29 Randolph Road, Hanscom AFB, MA 01731-3010. This will assist us in maintaining a current mailing list.

Do not return copies of this report unless contractual obligations or notices on a specific document requires that it be returned.

REPORT DOCUMENTATION PAGE

Form Approved
OMB No. 0704-0188

1. AGENCY USE ONLY (Leave blank)	2. REPORT DATE	3. REPORT TYPE AND DATES COVERED
	6/10/97	FINAL REPORT 06/15/95 - 06/14/97

4. TITLE AND SUBTITLE Development of Discrimination, Detection, and Location Capabilities in Central and Southern Asia Using Middle-Period Surface Waves Recorded by a Regional Array

5. FUNDING NUMBERS
F19628-95-C-0099
PE35999F
PR5101 TAGM
WU AJ

6. AUTHOR(S)
Anatoli L. Levshin
Michael H. Ritzwoller

7. PERFORMING ORGANIZATION NAME(S) AND ADDRESS(ES)
University of Colorado
Department of Physics
Campus Box 390
Boulder, CO 80309

8. PERFORMING ORGANIZATION REPORT NUMBER
1534715 - 06/10/97

9. SPONSORING/MONITORING AGENCY NAME(S) AND ADDRESS(ES)
Phillips Laboratory
29 Randolph Road
Hanscom AFB, MA 01731-3010
Contract Manager: James Battis/GPE

10. SPONSORING/MONITORING AGENCY REPORT NUMBER
PL-TR-97-2077

11. SUPPLEMENTARY NOTES

12a. DISTRIBUTION/AVAILABILITY STATEMENT
Approved for public release: Distribution unlimited

12b. DISTRIBUTION CODE

13. ABSTRACT (Maximum 200 words)

This report presents the results of a study of the dispersion characteristics of intermediate period broadband fundamental surface waves propagating across Central Asia, Western China, and parts of the Middle East. We present group velocity maps from 10 s to 40 s period for both Rayleigh and Love waves. Broadband waveform data from about 600 events from 1988 - 1995 recorded at 83 individual stations from several global and regional networks (MEDNET, KNET, KAZNET) have produced about 9,000 paths for which individual dispersion curves have been estimated. These data break into two sets of measurements: those from about 400 large ($M_s > 5.0$) earthquakes from around the continent recorded on both global and regional networks and those from about 200 additional smaller ($M_s \leq 5.0$) events recorded regionally at KNET and KAZNET. The combination of measurements on these two spatial scales helps to optimize path coverage and azimuthal distribution which together determine resolution. This study displays denser and more uniform data coverage and demonstrates higher resolution (~ 4°) than previous studies that have been performed on this scale and at these periods. The group velocity maps display the signatures of known geological and tectonic features never before revealed in surface wave studies on this scale, and provide a significant improvement in fit to the observed dispersion curves. These maps should prove useful to predict group travel times for the identification and extraction of surface wave packets, and to construct more accurate and detailed regional models of the lithosphere.

14. SUBJECT TERMS
Surface Waves Central Asia Tomography Crustal Structure
Regional Seismic Arrays

15. NUMBER OF PAGES
58

16. PRICE CODE

17. SECURITY CLASSIFICATION OF REPORT	18. SECURITY CLASSIFICATION OF THIS PAGE	19. SECURITY CLASSIFICATION OF ABSTRACT	20. LIMITATION OF ABSTRACT
Unclassified	Unclassified	Unclassified	SAR

Contents

Abstract

This report presents the results of a study of the dispersion characteristics of intermediate period fundamental surface waves propagating across Central Asia, Western China, and parts of the Middle East. We present group velocity maps from 10 s to 40 s period for both Rayleigh and Love waves. Broadband waveform data from about 600 events from 1988 - 1995 recorded at 83 stations from 'global' (GDSN, IRIS/GSN, GEOSCOPE, CDSN) and 'regional' networks (MEDNET, KNET, KAZNET) have produced about 9,000 paths for which individual dispersion curves have been estimated. These data break into two sets of measurements: those from about 400 large ($M_s > 5.0$) earthquakes from around the continent recorded on both global and regional networks and those from about 200 additional smaller ($M_s \leq 5.0$) events recorded regionally at KNET and KAZNET. The combination of measurements on these two spatial scales helps to optimize path coverage and azimuthal distribution which together determine resolution. The regional, small event data allow the period range of the estimated group velocity maps to be reduced. The tomographic method of Yanovskaya and Ditmar is used to estimate group velocity maps separately for each period and wave type (Rayleigh or Love). Resolution is estimated from 'checker-board' tests and we show that resolutions across most of the studied region are about 4°-5° at 20 s and above, but degrade at shorter periods. Resolution is far from uniform spatially, and is generally worst in Western and Southern Iran and in India. Many known geological and tectonic structures are observed in the group velocity maps. Of particular note are the signatures of sedimentary basins, continental platforms and shields, and crustal thickness variations due to mountain roots and deformation resulting from continental collisions. Comparison of the estimated group velocity maps with those predicted by the hybrid model CRUST-5.1/S16B30 is qualitatively very good, but, because of the coarseness of its grid, CRUST-5.1 misses some of the smaller sedimentary basins (e.g., Tarim Basin, Tadzhyk Depression) and the geometry of crustal thickening in Central Asia cannot be well represented by any gridded 5° model.

All data (dispersion measurements, group velocity maps) and preliminary shear velocity models are made available to the seismological community via our Eurasian Tomography Web Site at:

http://tagg.colorado.edu/geophysics/eurasia.dir/eurasia.html

1. Introduction

This report presents the results of a study of intermediate period (10 - 40 s) Rayleigh and Love wave dispersion across Central Asia, Western China, and regions of the Middle East. The studied region encompasses latitudes from 20°N to 50°N and longitudes from 45°E to 105°E and the focus of this report is on the estimation, presentation, evaluation, and interpretation of group velocity maps.

There are two main motivations for this study. First, accurate high resolution intermediate period group velocity maps are useful in monitoring clandestine nuclear tests. These maps guide the identification and extraction of surface waveforms which emanate from small seismic events. The estimation of surface wave magnitude, M_s, near 20 s period is thereby facilitated for use as part of, for example, the $M_s : m_b$ method of discriminating underground explosions from naturally occurring earthquakes (e.g., Stevens and Day, 1985). In addition, the existence of group velocity maps below 20 s period should allow for the development of a regional surface wave magnitude scale based on a shorter reference period so that the discriminant could be applied to smaller earthquakes and explosions. Second, regional intermediate period dispersion maps provide new constraints on the shear velocity structure of the crust and on crustal thickness. As Das and Nolet (1995) point out, since surface wave sensitivities compress into the crust at the short period end of our study, group velocity maps below 25 s period are particularly important to help resolve Moho depth from the average shear velocity of the lower crust in seismic inversions.

In a recent study (Ritzwoller and Levshin, 1997), we presented Rayleigh and Love wave group velocity maps on a larger spatial scale (all of Eurasia) and for a broader period band (20 - 200 s) than considered here. There have also been other studies on larger scales and at longer periods that have produced dispersion maps (usually phase velocities) across the studied region; e.g., Feng and Teng (1983), Montagner and Tanimoto (1991); Trampert and Woodhouse (1995), Laske and Masters (1996), Zhang (1996), Ekstrom *et al.* (1997), and Curtis and Snieder (1997). In the current report, we discuss early attempts to provide improved resolutions on a regional scale and to extend the group velocity images to shorter periods. The success of these attempts depends on several factors:

- the use of data from regional networks and arrays in addition to global seismic network data;

- the use of data from events which are smaller in magnitude than those used on a continental scale, (i.e., $M_s \leq 5.0$);
- the combination of measurements made on paths that propagate continental-wide with those made on paths confined to the region of study.

Toward these ends, we have processed data from two networks in Kirghistan and Kazakhstan, KNET (Pavlis *et al.*, 1994; Vernon, 1994) and KAZNET (Kim *et al.*, 1995), following about 200 events with $M_s \leq 5.0$ which occurred largely within the studied region. These data are used in concert with measurements on records from stations distributed continent-wide which follow about 400 larger earthquakes dispersed around the continent, most with $M_s \geq 5.5$. The use of these 'short-path' measurements is mostly intended to help reduce the period range of the study, but also helps to improve resolution in the studied region. The combination of these measurements with 'long-path' measurements helps to improve the homogeneity of ray path coverage and to provide crossing paths, both of which improve resolution and work to reduce sensitivity to event mislocation.

The outline of the report is as follows. Section 2 presents a brief discussion of the data used in the study, the method of measurement used to produce the estimated group velocity curves, and the tomographic method used to translate the measured group velocity curves into group velocity maps at each period and for each wave type (Rayleigh or Love). These issues are discussed in greater detail by Ritzwoller and Levshin (1997). Section 3 presents a discussion of the resolution expected in the estimated group velocity maps. A sampling of the estimated group velocity maps is presented in Section 4 and they are discussed in Section 5. In particular, the discussion concentrates on comparing the estimated maps with group velocity maps predicted from the hybrid model composed of the crustal model CRUST-5.1 of Mooney *et al.* (1996) together with the mantle model S16B30 of Masters *et al.* (1996). A brief discussion of the geological features observed on the estimated group velocity maps is included here, and is discussed in more detail by Ritzwoller and Levshin (1997).

2. Data, Measurement, and Surface Wave Tomography

The data and the methods used to make the dispersion measurements, to estimate measurement uncertainties, and to translate the measurements into group velocity maps are

discussed in detail in Ritzwoller and Levshin (1997). A brief overview follows.

Data have been accumulated across Eurasia from the GDSN, GSN, CDSN, GEOSCOPE, MEDNET, KNET, and KAZNET seismic networks. Group travel time, phase travel time, and spectral amplitude measurements are obtained by use of an interactive Frequency-Time ANalysis (FTAN) method (e.g., Levshin *et al.*, 1972; Russell *et al.*, 1988; Levshin *et al.*, 1992; Ritzwoller *et al.*, 1995). Group velocity and phase velocity are computed from the distance between the receiver and the CMT location (Dziewonski *et al.*, 1981) when it exists, or the PDE location otherwise. As part of FTAN, an analyst interactively designs a group velocity - period filter to reduce contamination from other waves and coda, chooses the frequency band for each measurement, and assigns a qualitative grade (A - F) to each measurement. Data from approximately 600 events across Eurasia, most with $M_s \geq 5.0$, have been processed in this way to yield more than 9,000 measured Rayleigh wave dispersion curves and more than 7,600 Love wave dispersion curves across the continent. These numbers include data from about 200 smaller events ($4.0 < M_s \leq 5.0$) which occurred mostly in the studied region and which were processed only at KNET and KAZNET. The locations of stations and events used are shown in Figure 1.

The resulting data set exhibits considerable redundancy, which allows for consistency tests, outlier rejection, and the estimation of measurement uncertainties. The use of broad-band regional network data, such as those from KNET or KAZNET, are particularly useful for this purpose. Figure 2a shows two record sections, one for a large event in the Kurile Islands observed at GSN and CDSN stations and the other for a much smaller event in Western China observed at KNET. Measurements from similar paths are 'clustered' and compared. Paths are considered 'similar' if their starting and ending points both lie within 2% of the path length from one another. For example, for an event ~1850 km from KNET, like the Qinghai event of Figure 2a, measurements are clustered if stations lie within ~40 km of each other. Typically, measurements from two to three stations within KNET cluster for such short paths, but more stations within KNET cluster for longer paths. Measurements made at KAZNET are less likely to cluster since the network covers a larger area. About one-third of all measurements form part of some cluster. If a measurement at a specified period and wave type results from a cluster, the uncertainty assigned to it is the standard deviation of the measurements that form that cluster (at that period and wave type). For measurements

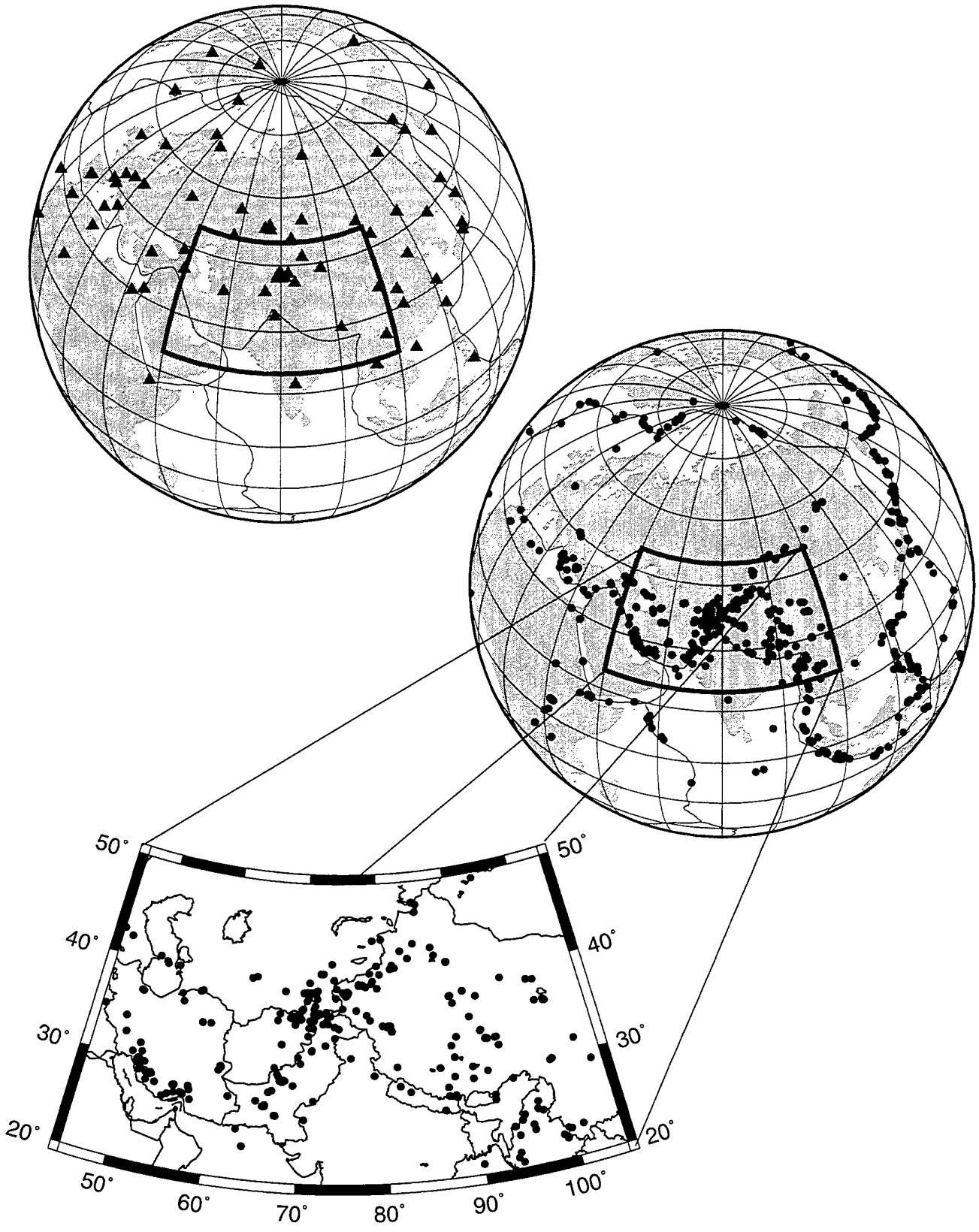

Figure 1. Station and event locations. The locations of the stations used in this study across Eurasia are marked with triangles at top and event locations are marked with circles in the middle. At bottom, a blow up of event locations in the region of study are shown.

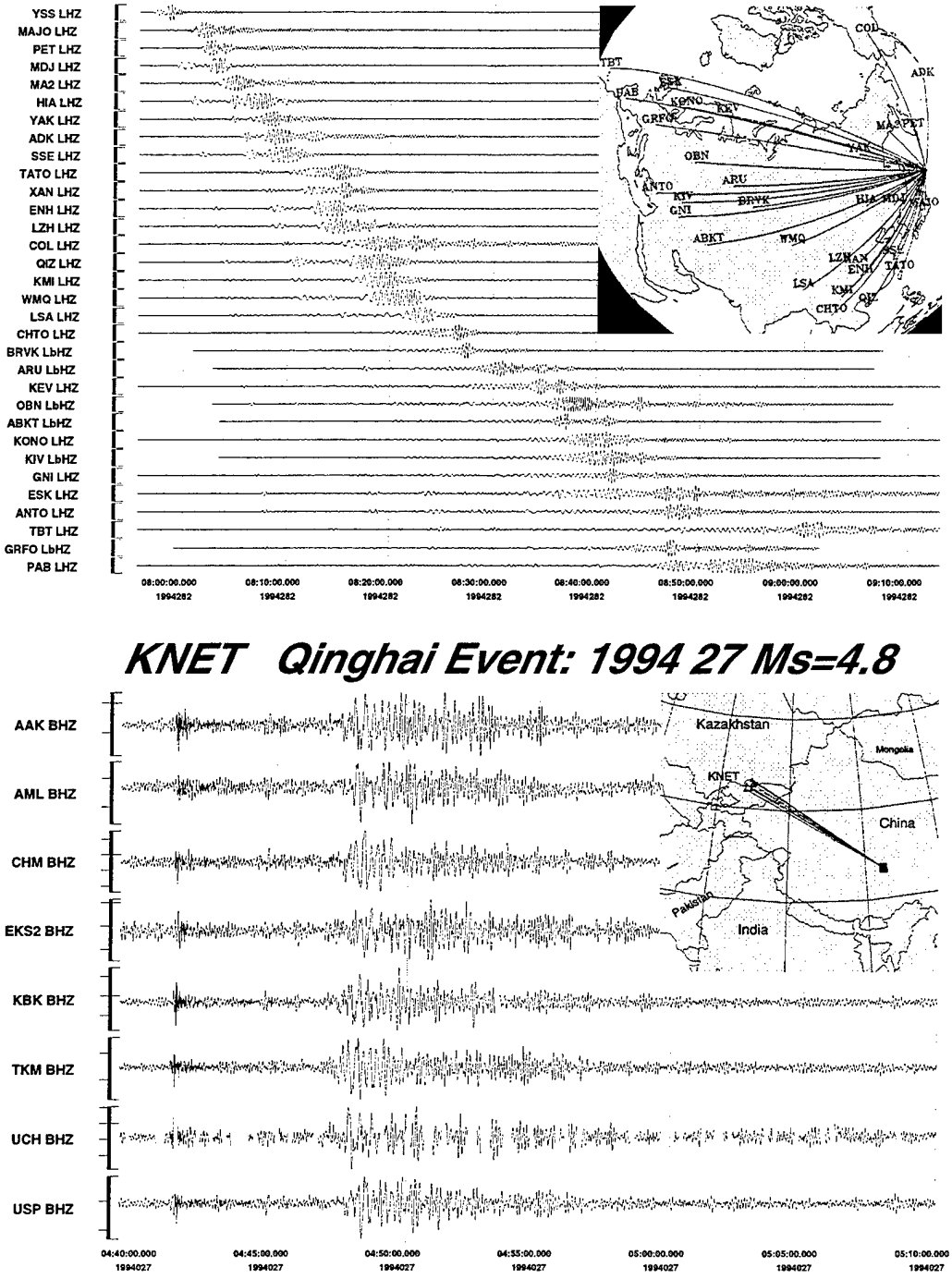

Figure 2a. (Top) Record section of IRIS/GSN vertical waveforms recorded following a large event in the Kurile Islands (10/9/95; Ms = 7.0). Waveforms have been low pass filtered with a lower corner of 20 s period. Ray paths are inset. (Bottom) Record section of KNET vertical waveforms for an intermediate sized event in Qinghai, China (1/27/94; Ms = 4.8)

that are not part of some cluster, the average of the standard deviations at that period and wave type taken over all clusters is assigned. Average measurement uncertainties estimated in this way are displayed if Figure 2b. They are about 0.04 km/s at 20 s period and above, but are much larger at shorter periods.

The algorithm of Ditmar and Yanovskaya (1987) and Yanovskaya and Ditmar (1990) is used to construct the group velocity maps. (See also Levshin *et al.*, 1989, Ch. 6.) This method estimates a group velocity map $U(\theta, \phi)$ at each period and wave type by attempting to minimize the following penalty function:

$$\sum_{i=1}^{N}[w_i(t_i^{obs} - t_i^{pred})]^2 + \lambda \int_S |\nabla U(\theta, \phi)|^2 dA, \tag{1}$$

where

$$t_i^{pred} = \int_{p_i} U^{-1}(\theta, \phi) ds. \tag{2}$$

Here, p_i represents the i-th wave path. w_i is the weight associated with the i-th path, $w_i = \sqrt{m}(g_i/\sigma_i)$, where m is the number of raw measurements that compose the cluster that produced this measurement, σ_i is the uncertainty determined from the cluster analysis for measurement i, and g_i is a weight which depends on the qualitative grade assigned to the measurement by the analyst (A-1.0, B-0.75, C-0.4, D-0.2, E-0.0, F-0.0). t_i^{obs} and t_i^{pred} are the observed and the predicted group travel times along the i-th path and S is the region on which the inversion is performed. Choosing different values of the trade-off parameter, λ, changes the trade-off between the fit to the data and the 'smoothness' of the resulting group velocity map. 'Smooth' here is defined in terms of the spatial gradient of the model. The trade-off parameter is chosen by analyzing misfit and the visual characteristics of the resulting maps. Typically, λ is chosen to produce a slightly underdamped map and, since the penalty function in equation (1) does not include a second-spatial gradient term, each map is smoothed a posteriori with a Gaussian spatial-smoothing filter whose width derives from the resolution analysis (described in Section 3). In practice, we apply a smoothing filter whose full width at e^{-1} of its maximum height is one-half the estimated resolution. Both the resolution analysis and inversion take place separately for each period and wave type. In equation (2), we assume that each wave path, p_i, is along the great-circle linking the source and receiver and no group time perturbation is introduced by a source group time shift (e.g., Knopoff and Schwab, 1968; Levshin *et al.*, 1997). This algorithm is discussed more thoroughly by Ritzwoller and Levshin (1997).

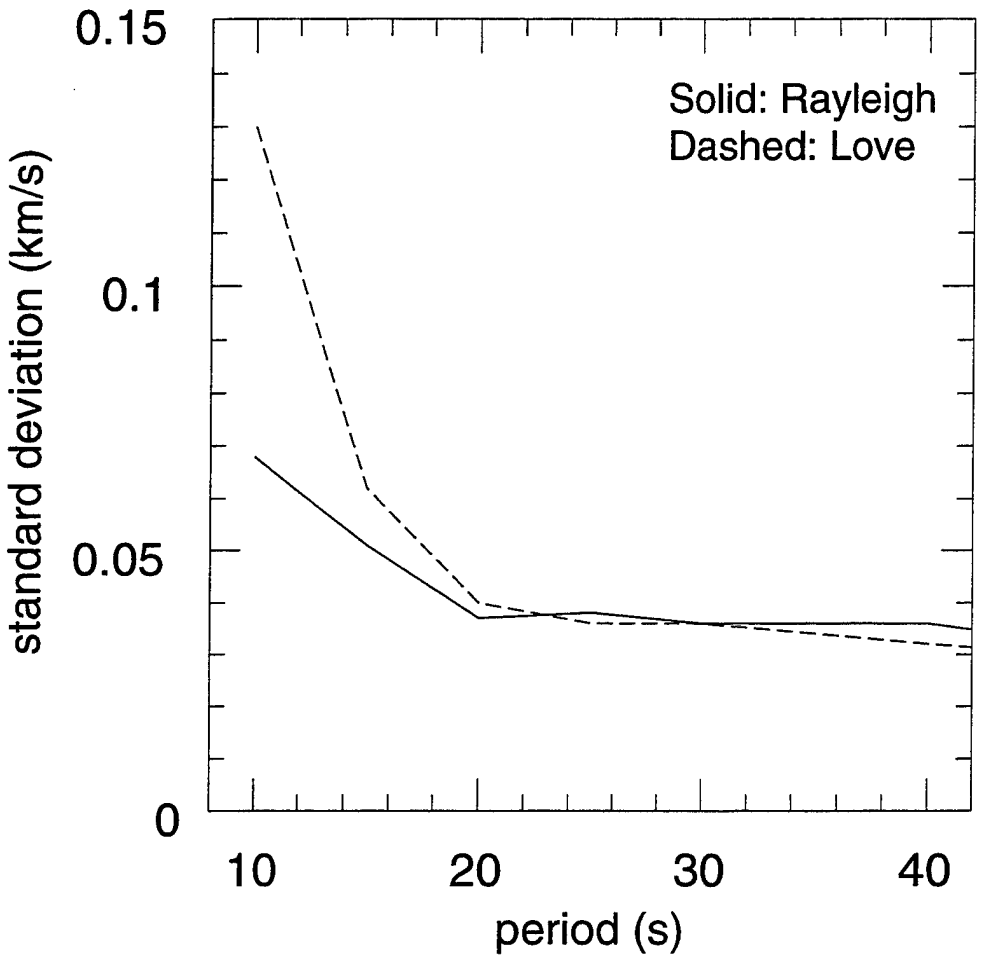

Figure 2b. Average measurement uncertainty estimated from the cluster analysis. Solid line - Rayleigh wave, dashed line - Love wave.

3. Resolution Analysis

The resolution of the data set depends strongly on geographical location, period, and wave type. Experience shows that all three of the following are required to produce a resolution of 5° or less: high path density, good azimuthal coverage, and a significant number of paths shorter than ~30°. In this section, we present the results of a standard 'checkerboard' resolution analysis and show that, on average, resolution across much of the studied region is about 4°-5° at periods of 20 s and above. However, resolution degrades sharply below 20 s period. We argue here that the reason for this degradation is that most measurements below 20 s period are from paths entirely contained within the studied region. Figure 3 shows histograms depicting the number of paths as a function of path length, period, and wave type. The shortage of paths that either originate or end outside of the studied region severely limits azimuthal coverage which reduces the accuracy and resolution of the group velocity maps below 20 s period. For this reason, the quality of the group velocity maps shown in Section 4 is highly variable. In interpreting the estimated group velocity maps it is important to refer to the resolution analyses presented in this section.

Examples of path density are shown in Figures 4a and 4b where we plot the number of paths that intersect each square two° cell (~50,000 km^2). Path densities are highest in the interior of the studied region, usually maximizing near KNET, and decrease toward the south at all periods and towards the north below 20 s period. Below about 20 s period, most of the measurements are for paths entirely withing the region of study, as Table 1 indicates. For example, for the 15 s Rayleigh wave there are 756 paths through the region of study and 510 of these are contained entirely within this region. However, for the 30 s Rayleigh wave, there are 2684 measurements through the region, of which only 469 are from paths contained entirely within the studied region. Thus, at periods below 20 s, path distribution is dominated by station and event distribution within the studied region and is, therefore, less homogeneous than the distribution of paths at longer periods. For example, at 10 s and 15 s period, there are few paths constraining India, Central China, the Persian Gulf region, or the Caspian region. In addition, the azimuthal distribution of paths below 20 s period is less complete than at longer periods. Below 20 s period, path distribution is dominated by measurements made at KNET from events in Western China (to the southeast of KNET) and in Southern Iran (to the southwest of KNET). This produces the characteristic

Table 1. Path Information about Measurements

	Rayleigh Waves			Love Waves		
period	*within region*[1]	*touching region*[2]	*total*[3]	*within region*[1]	*touching region*[2]	*total*[3]
10 s	416	438	448	254	276	287
15 s	510	756	1091	369	526	794
20 s	523	1420	2068	375	1029	1882
25 s	494	2168	4249	378	1718	3182
30 s	469	2684	5116	370	2292	4181
40 s	359	2898	5349	294	2529	4590

1 - number of paths which are entirely contained within the studied region

2 - number of paths which at least touch the studied region

3 - total number of paths across Eurasia, including those that do not touch the studied region

Table 2a. Resolution Analysis at 20 s Period: Percentage of Cells in Each Resolution Category (All Paths)

	Rayleigh Wave			Love Wave		
cell size	*not resolved*	*nearly resolved*	*resolved*	*not resolved*	*nearly resolved*	*resolved*
3° cells	35%	26%	39%	44%	21%	35%
5° cells	12%	4%	84%	16%	15%	69%
7.5° cells	0%	3%	97%	6%	0%	94%
10° cells	0%	0%	100%	0%	4%	96%

Table 2b. Resolution Analysis at 20 s Period: Percentage of Cells in Each Resolution Category (Paths Within Region)

	Rayleigh Wave			Love Wave		
cell size	*not resolved*	*nearly resolved*	*resolved*	*not resolved*	*nearly resolved*	*resolved*
3° cells	77%	12%	11%	85%	10%	5%
5° cells	65%	9%	26%	68%	12%	20%
7.5° cells	53%	17%	30%	58%	17%	25%
10° cells	36%	18%	46%	36%	18%	46%

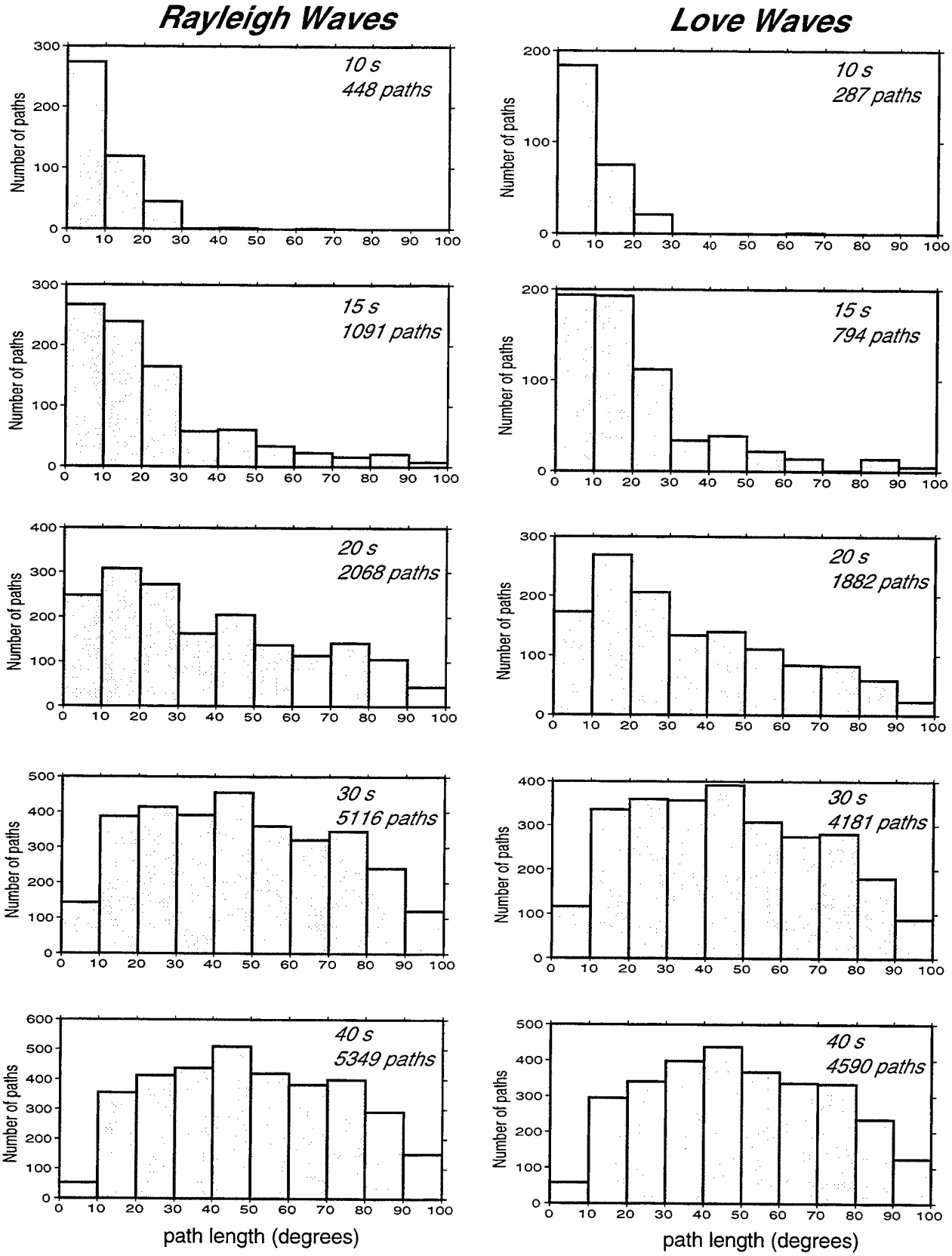

Figure 3. Histograms displaying the number of dispersion measurements (after the cluster analysis) for all paths that touch the studied region, as a function of path length segregated by period ranging from 10 - 40 s. Left column: Rayleigh waves; Right column: Love waves.

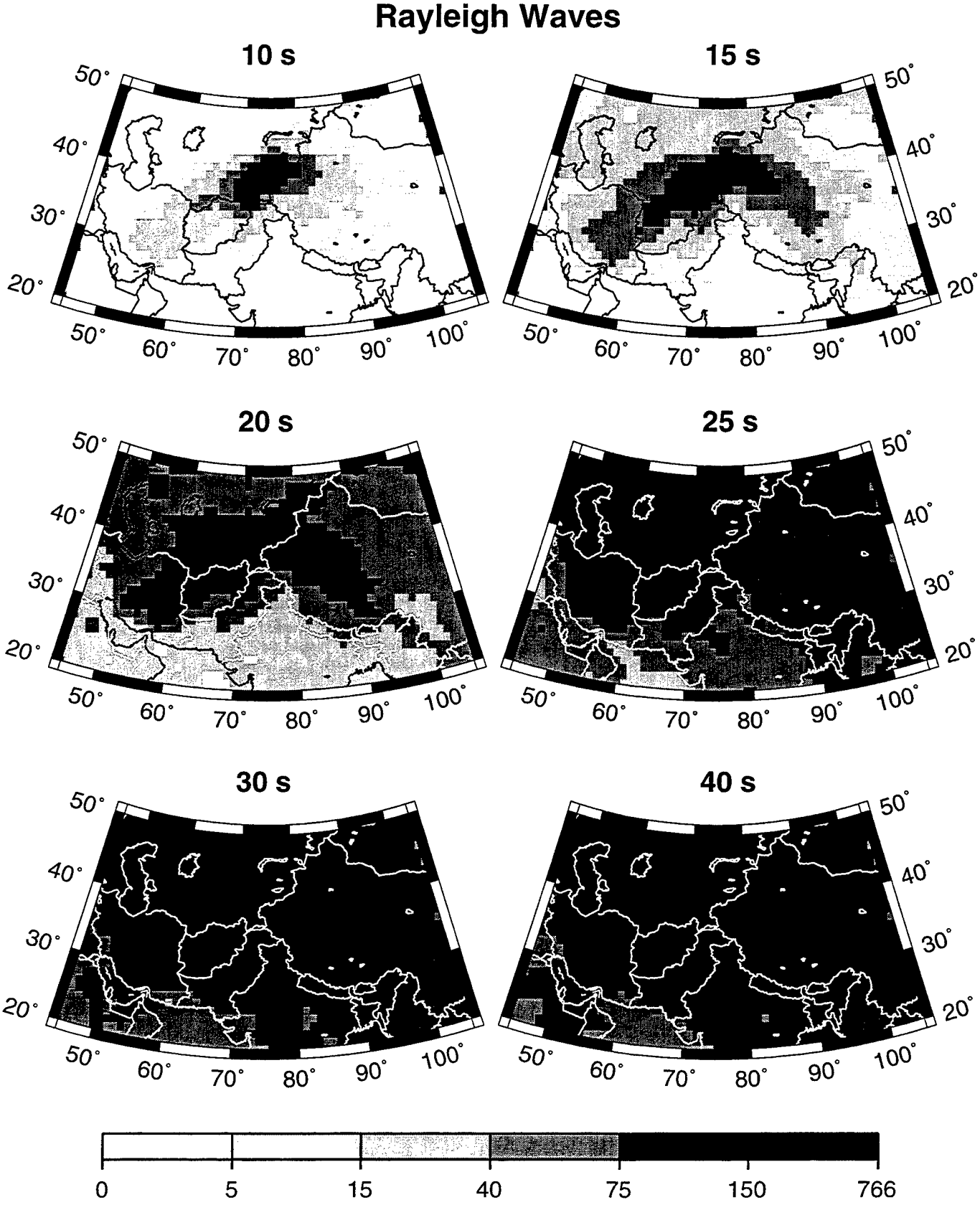

Figure 4a. Path density for Rayleigh waves at the six indicated periods. Path density is defined as the number of rays intersecting a 2 degree square cell (~50,000 sq. km).

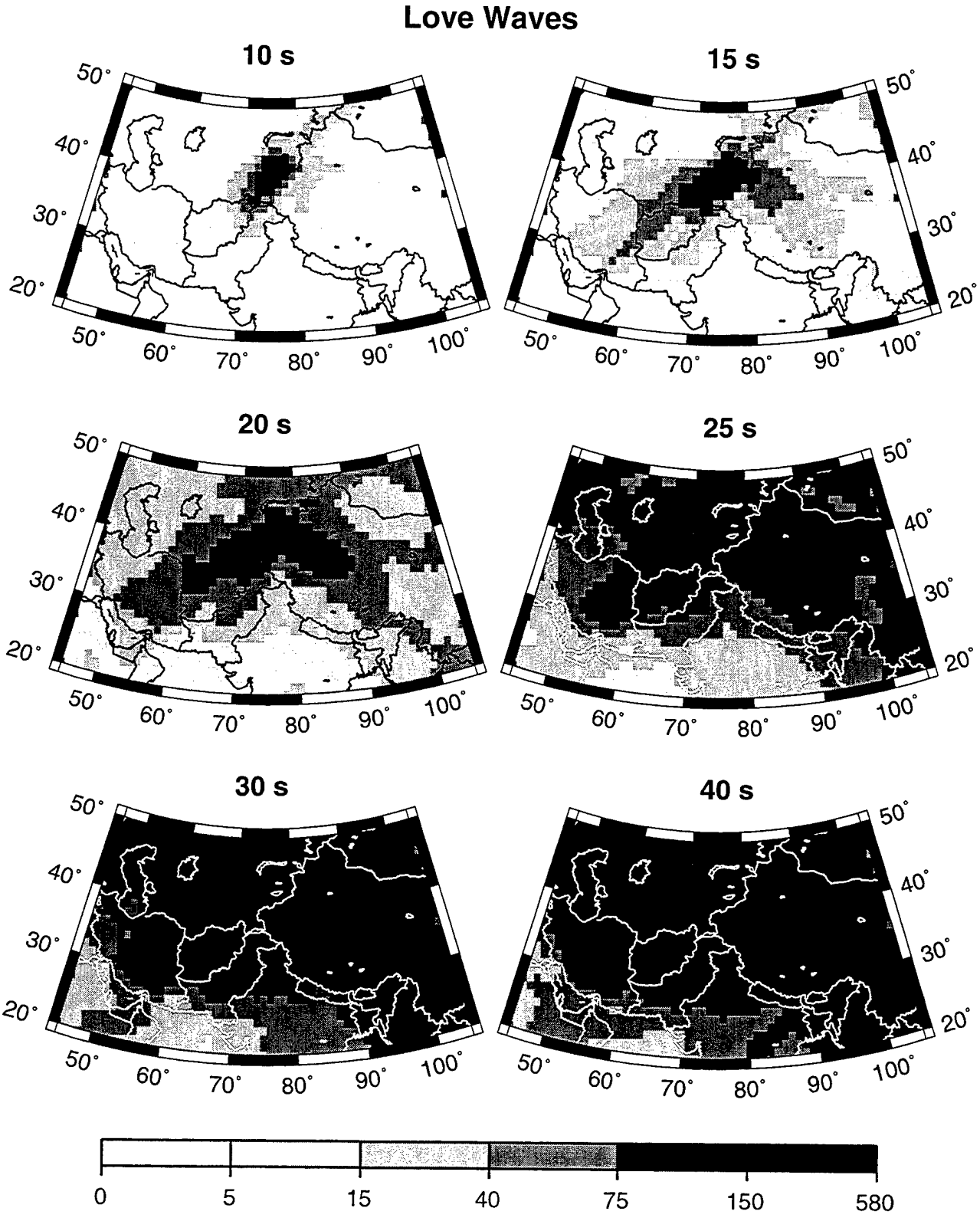

Figure 4b. Same as Figure 4a, but for Love waves at the indicated periods.

northwest-southeast and southwest-northeast stripes that appear on the plots of path density and resolution at short periods. At 20 s period and above, measurements from the paths that begin or end outside of the studied region come into play, as Figure 3 shows, and this improve coverage appreciably.

To estimate resolution we perform a standard 'checker-board' test. Each model is divided into cells of equal area with each cell possessing a velocity perturbation of $\pm 10\%$ of the average across each map. Travel time perturbations are accumulated along the great circle linking each source and receiver. We estimate resolution as a function of wave type and period by computing synthetic travel times through the checker-board model for exactly the paths that have emerged from the cluster analysis and then inverting these synthetic data using the same weighting and damping used in the group velocity tomography described in Section 2.

Checker-board plots at the resolutions of this study (3° - 5°) are difficult to interpret since the cells are very small. To simplify interpretation, we assign a 'Resolution Index', $\mathcal{R}_i$, to each cell:

$$\mathcal{R}_i = \frac{v_{\max}}{v_{\text{input}}} \qquad \text{(in percent)}. \tag{3}$$

Here, $v_{\max}$ is the estimated velocity perturbation whose absolute value is maximum in the cell and v_{input} is the input velocity perturbation in the same cell ($\pm 10\%$). Perfect resolution would result in $\mathcal{R}_i = 100\%$, poor resolution results in $\mathcal{R}_i \leq 30\%$. The resolution index can be less than zero if the sign of $v_{\max}$ is opposite from the input value of the cell or greater than 100% if the estimated magnitude is higher than the input value.

In Figures 5 - 7, we plot resolution indices for a variety of cell sizes, periods and wave types. A cell is considered resolved if $\mathcal{R}_i > 50\%$ in which case then the cell is shaded light grey. The regions with poorer resolutions are indicated by the darker cells. In Figures 5a and 5b, resolution index is plotted for the 20 s Rayleigh and Love waves for a variety of cell sizes ranging from 3° to 10°. In general, Rayleigh wave resolution is better than Love wave resolution. We say that the region of study has a given resolution if more than 50% of the cells in that region are resolved. As Table 2a indicates, more than 50% of the 5° cells are resolved for both the Rayleigh and Love waves at 20 s period if all the data are used, and we claim a resolution of 5° for both Rayleigh and Love waves at 20 s period. Resolution is worst

20 s Rayleigh Wave

all paths

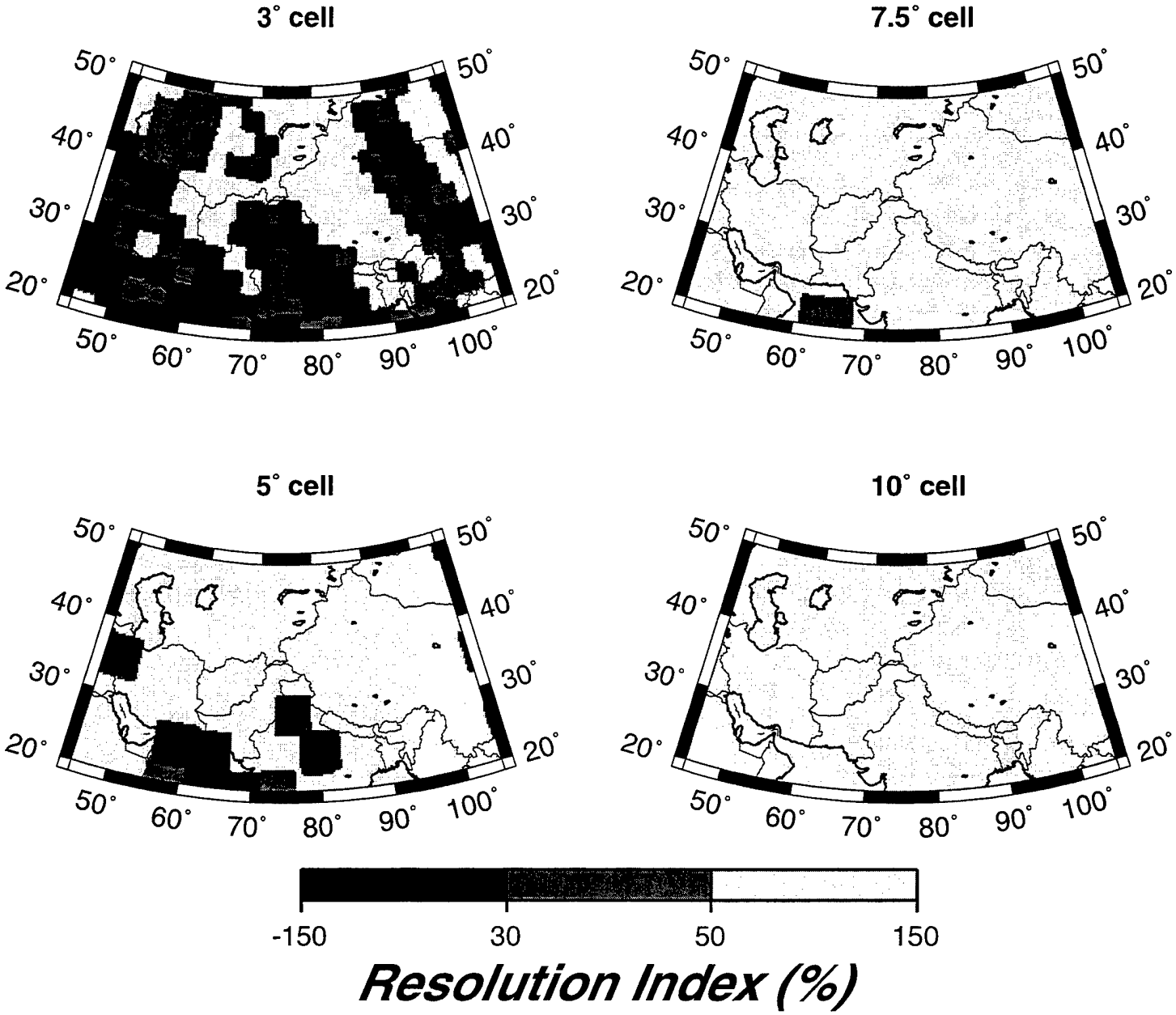

Figure 5a. Plots of resolution index ($\Re$, eqn. (3)), for the 20 sRayleigh wave for four cells sizes: 3°, 5°, 7.5°,and 10°. Three grey-scale values are presented, the lightest indicates what we consider to be good resolution, increasingly dark cells reveal poorer resolutions.

20 s Love Wave

all paths

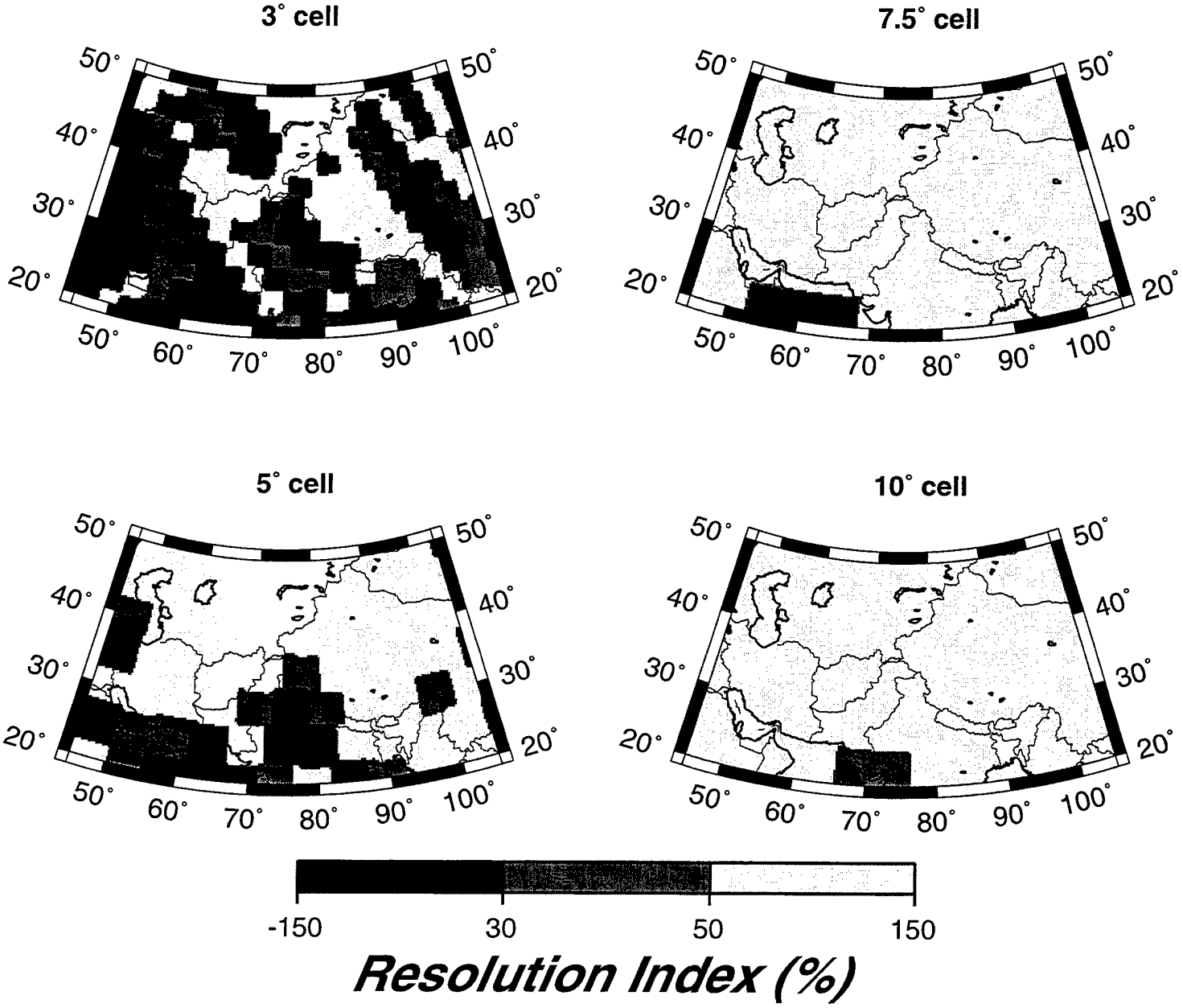

Figure 5b. Same as Figure 5a, except for Love waves at 20 s period.

at 20 s period in Northern India, parts of Pakistan, Northwestern Iran and the Southern Caspian, parts of the Persian Gulf, and the Arabian Sea. These are the regions most poorly resolved at all periods, consistent with the observations of path distribution discussed above.

Resolution is worsened considerably if only paths from within the studied region are used, as Figures 6a and 6b show. A comparison of Figures 5 and 6 demonstrates the importance of using group velocity measurements from paths that originate or terminate outside the studied region. The use of such paths improves the homogeneity of path distribution and azimuthal coverage, and, hence, improves resolution. Table 2b indicates that if only short-path data are used, 50% of the cells are not resolved even for 10° cells.

Figures 7a and 7b show the resolution index plots for 5° cells at periods of 10 s, 15 s, 30 s and 40 s for Rayleigh and Love waves, respectively. The northwest-southeast and northeast-southwest striping that appears in the path density maps also is apparent in the resolution maps at 10 s for both Rayleigh and Love waves and for the 15 s Love wave. The cell size at which at least 50% of the studied region appears resolved is plotted in Figure 8.

An assumption at the heart of all resolution analyses is that the resolution and accuracy of the estimated dispersion maps are dominated by known quantities that can be simulated in the resolution analysis: e.g., measurement uncertainties, path coverage, and damping used in the inversion. However, theoretical errors, which may be of unknown magnitude, also affect resolution. Such errors include event mislocation, azimuthal anisotropy, off-great-circle propagation, and source group time shifts. Ritzwoller and Levshin (1997) and Levshin *et al.* (1997) argue that these phenomena should not produce errors larger than those reported in the resolution analysis across the studied region at the periods considered in this study. In particular, they point out that the use of measurements from paths that begin and/or end outside the studied region reduces sensitivity to event mislocations in the region of study. This is yet another reason why regional tomographic studies are best performed as a focused part of a larger scale study. For these reasons, we believe that the resolution analyses accurately represent uncertainties in the estimated group velocity maps. That is, on averge, theoretical errors should not produce amplitude biases larger than 50% and geographical biases greater than the stated resolution.

20 s Rayleigh Wave

paths within region

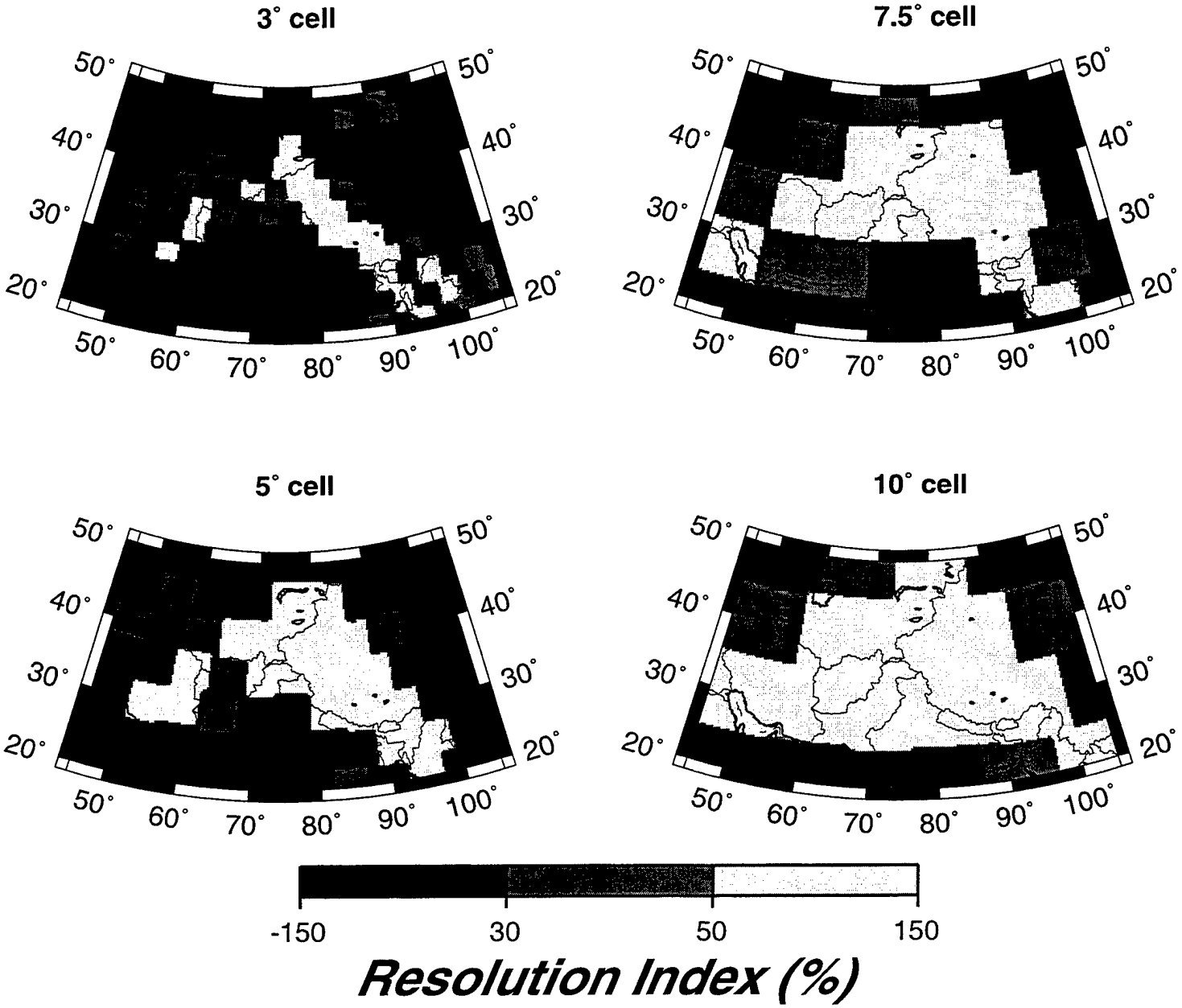

Figure 6a. Same as Figure 5a, except only paths entirely contained within the studied region are used. There are 523 such measurements for the 20 s Rayleigh wave, compared to a total of 1420 measurements if paths that originate and/or terminate outside the studied region are also used.

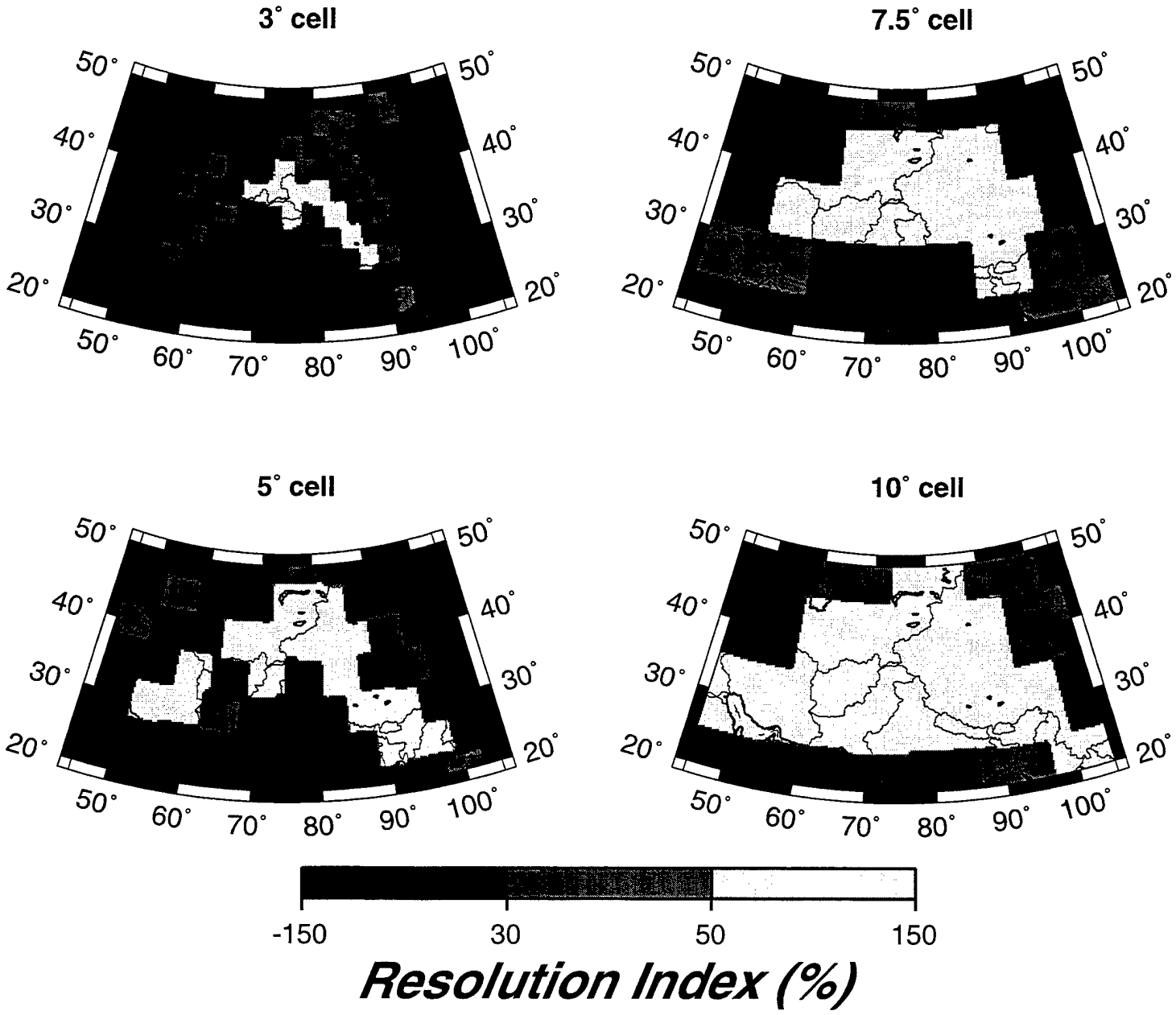

Figure 6b. Same as Figure 6a, except for Love waves.

Rayleigh Waves

5° cells

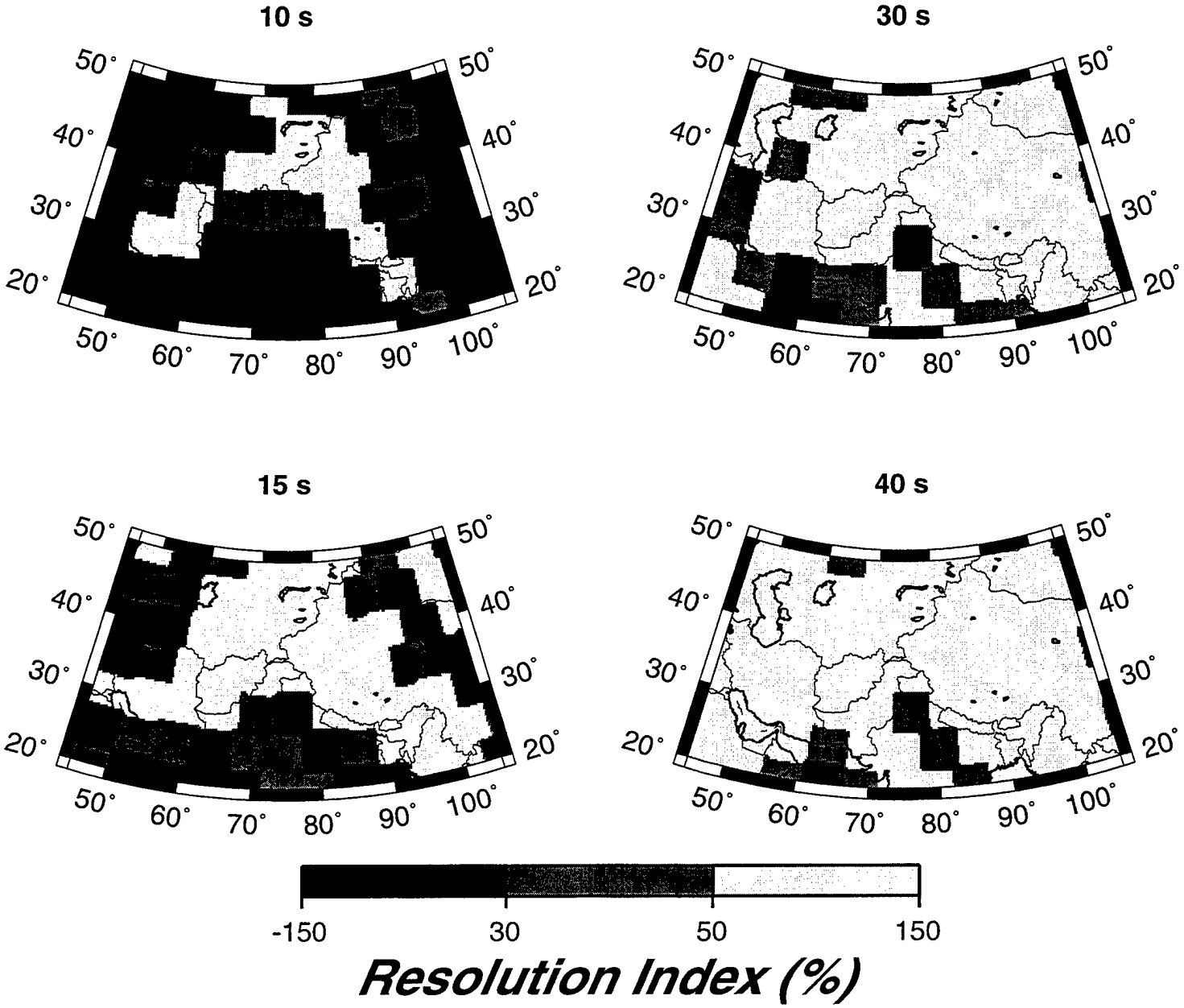

Figure 7a. Resolution index ($\Re$, eqn.(3)) plotted for Rayleigh waves at the indicated periods for 5° cells.

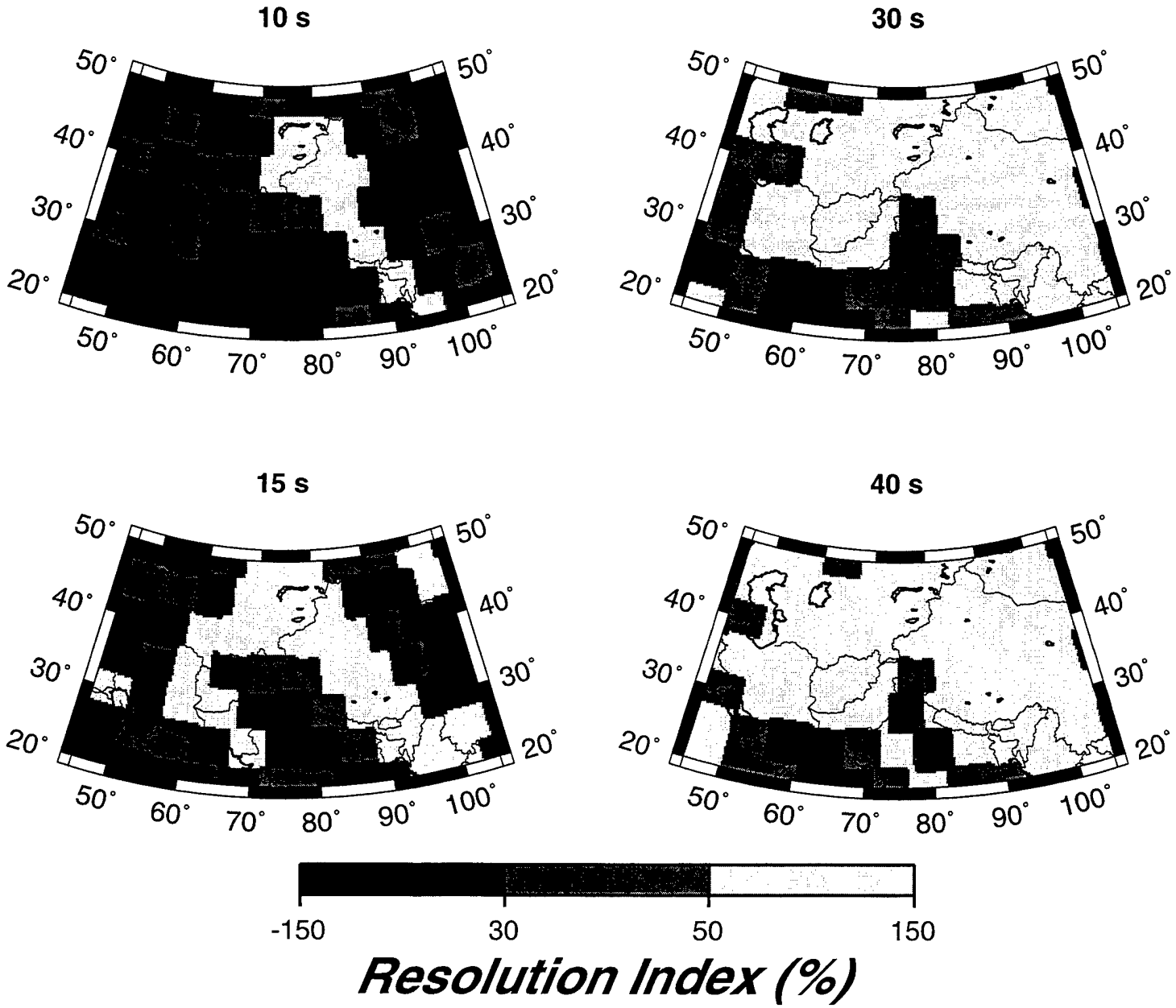

Figure 7b. Same as Figure 7a, but for Love waves at the indicated periods.

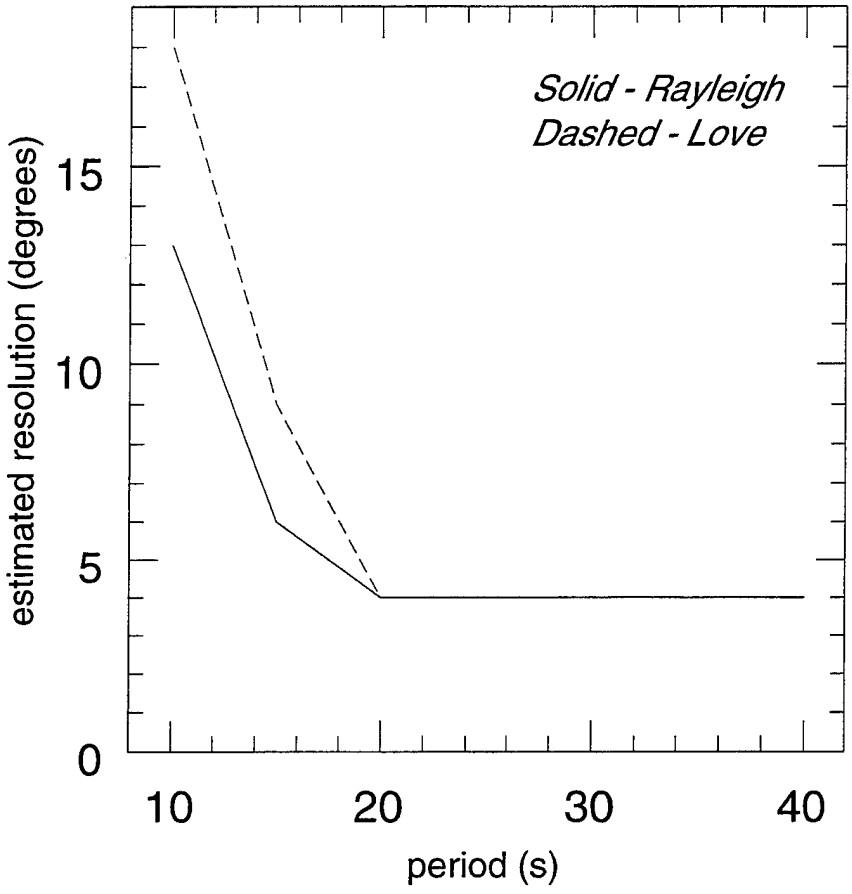

Figure 8. Estimated average resolution across the region of study. The value of resolution is chosen such that most (i.e., > 50%) of the studied region appears to be resolved in 'Resolution index' plots, such as those shown in Figures 5 and 7.
Certain regions may display better or worse resolutions than indicated here depending on if the path density and/or azimuthal coverage of the measurements that constrain the region are better or worse than average.

4. Group Velocity Maps

Using the tomographic method described in Section 2, we construct group velocity maps, which are smoothed using the estimated average resolution presented in Figure 8, for Rayleigh and Love waves at the following periods: 10, 15, 20, 25, 30, 40 s. Group velocity curves that represent the average of the group velocity maps across the studied region (latitude bounds: 20°N - 50°N; longitude bounds: 45°E - 105°E) for Rayleigh and Love waves are plotted in Figure 9. Comparison is made with the group velocity curves predicted from PREM (Dziewonski and Anderson, 1981) and the average of a hybrid aspherical model of the crust (CRUST-5.1: Mooney *et al.*, 1996) and mantle (S16B30: Masters *et al.*, 1996) across the studied region.

A sampling of the estimated group velocity maps is presented in Figures 10 and 11. These maps represent lateral group velocity variations relative to the regional average shown in Figure 9. In Figure 10, 20 s Rayleigh and Love wave group velocity maps are shown which have been constructed with data from paths entirely contained within the studied region. In Figures 11a - 11f, group velocity maps from 10 - 40 s period are shown for both Rayleigh and Love waves using all data that cross the studied region. A comparison of Figure 10 with Figures 11b and 11e for the 20 s Rayleigh and Love waves indicates what was also apparent from the resolution analyses shown in Figures 5 and 6 using these two different data sets. Much more accurate and more highly resolved group velocity maps are produced if short path data from within the region of study are combined with longer path data that originate and/or terminate outside the studied region.

Figure 12 shows the fit to the measured dispersion curves delivered by the estimated group velocity maps expressed as two different measures of misfit. The first is variance reduction relative to PREM:

$$\text{Variance Reduction} = 1 - \frac{\sum_i (U_i^{obs} - U_i^{pred})^2}{\sum_i (U_i^{obs} - U_0)^2}, \tag{4}$$

where i is the path index, U_i^{pred} is the predicted group velocity for path i through the estimated group velocity map shown in Figure 11, U_i^{obs} is the measured group velocity for path i, and U_0 is the reference group velocity from PREM. The second measure of misfit is

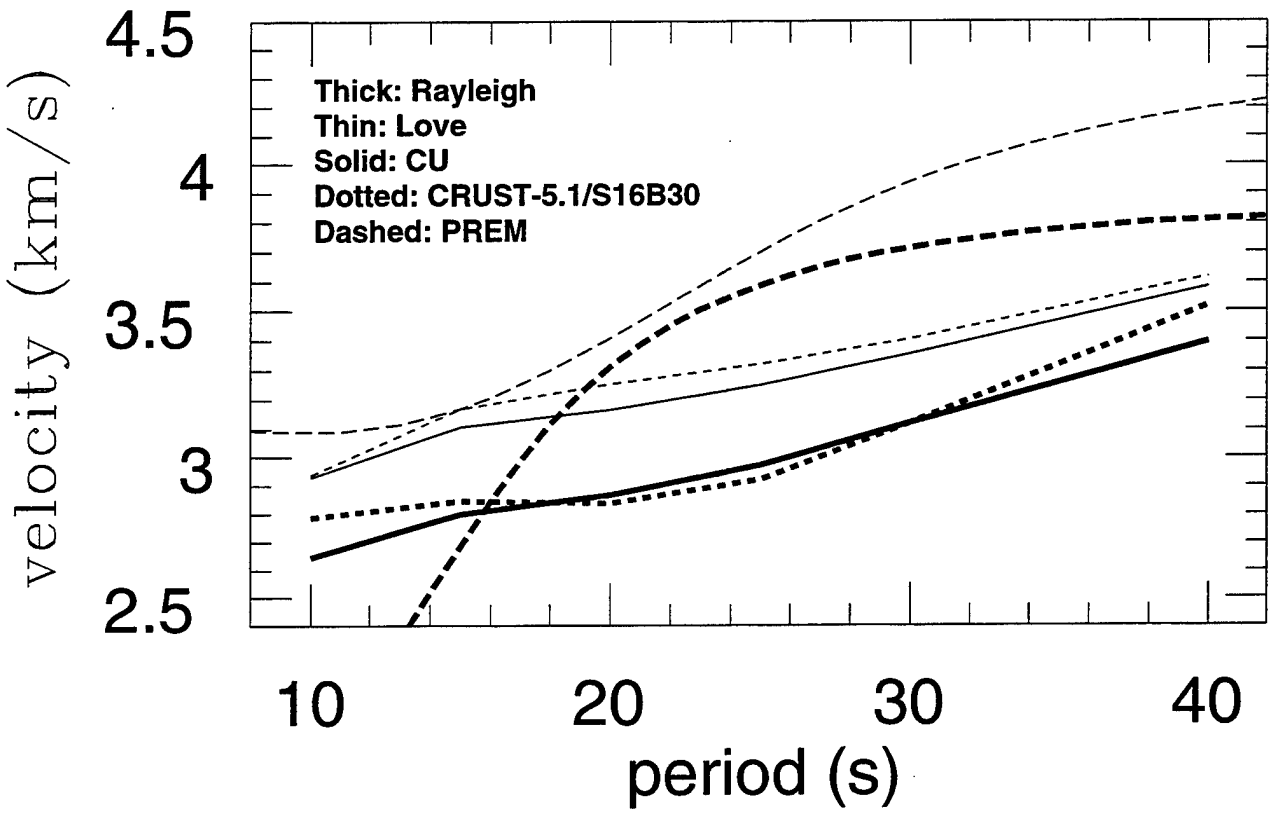

Figure 9. Average group velocity curves across the region of study (latitude: 20N - 50N, longitude: 45 - 110E) for our estimated group velocity maps (CU: solid lines), PREM (PREM: long dashed line), and the group velocity maps predicted by a model composed of the crustal model CRUST-5.1 and the mantle model S16B30 (CRUST-5.1/S16B30: short dashed line). Rayleigh waves are the thick lines, Love waves are the thin lines.

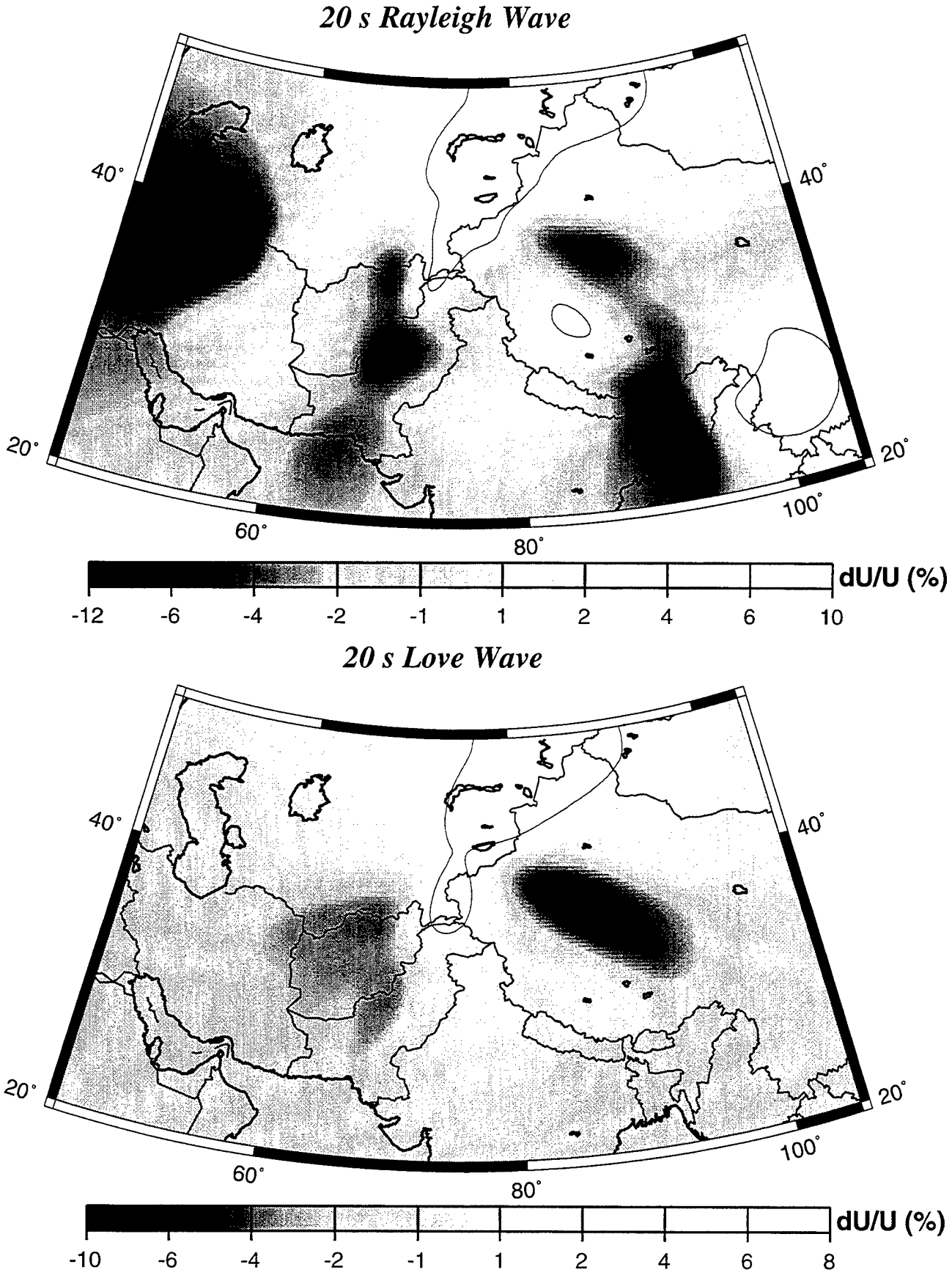

Figure 10. Group velocity maps for the 20s Rayleigh and Love waves constructed using measurements from paths entirely contained within the region of study.

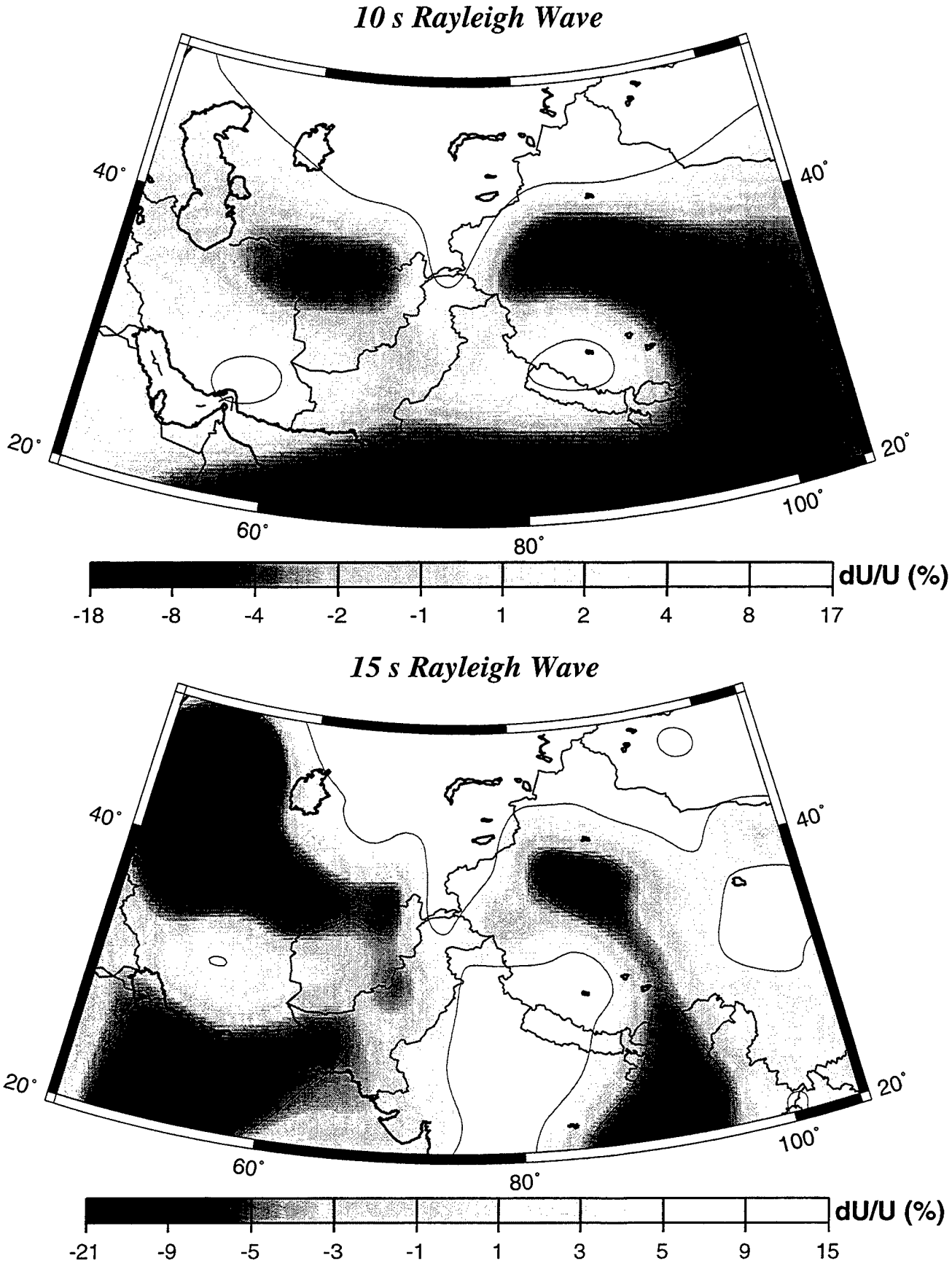

Figure 11a. Estimated group velocity maps for the 10 s and 15 s Rayleigh waves. (All paths are used.)

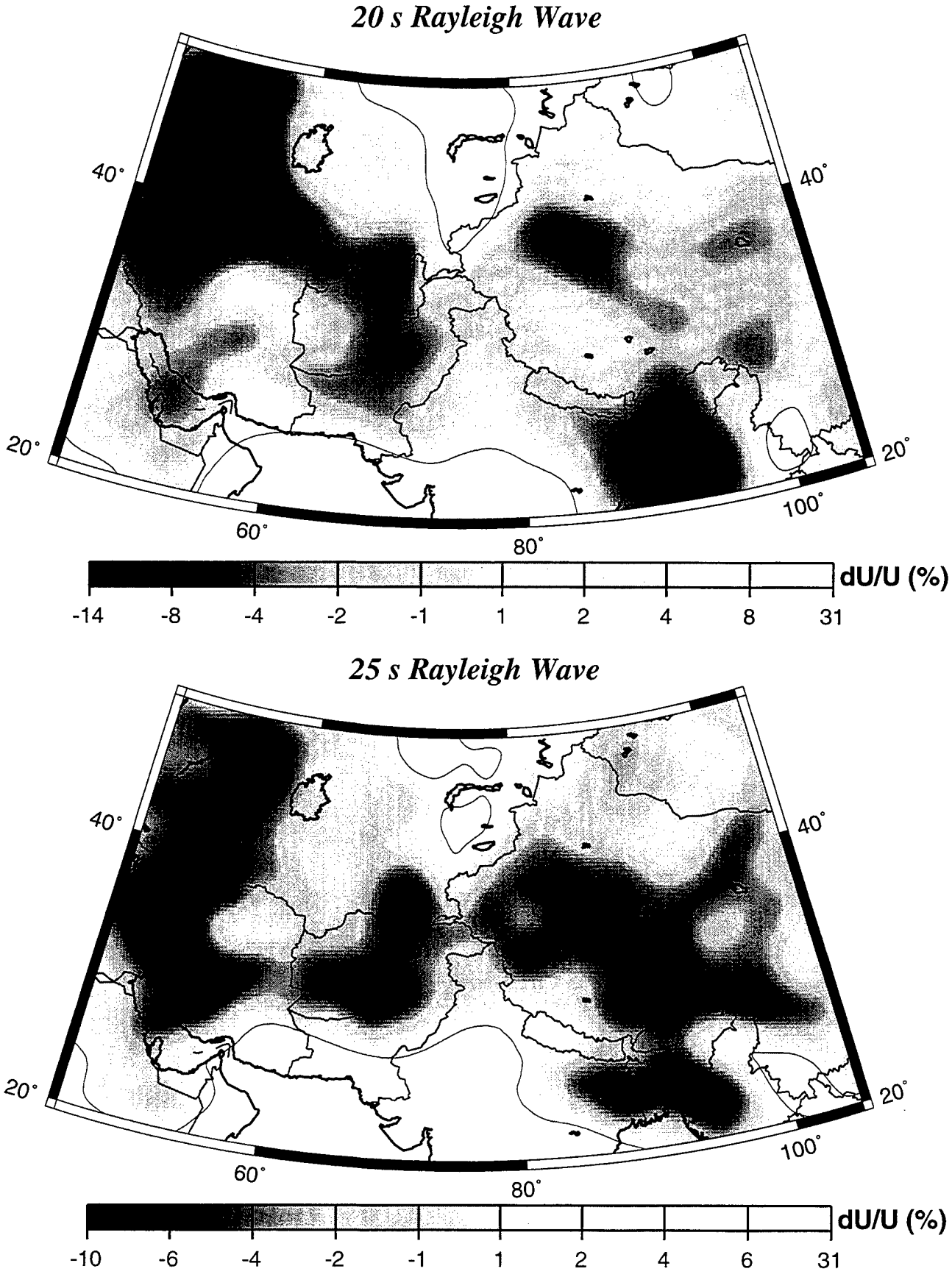

Figure 11b. Same as Figure 11a, but for the 20 s and 25 s Rayleigh waves.

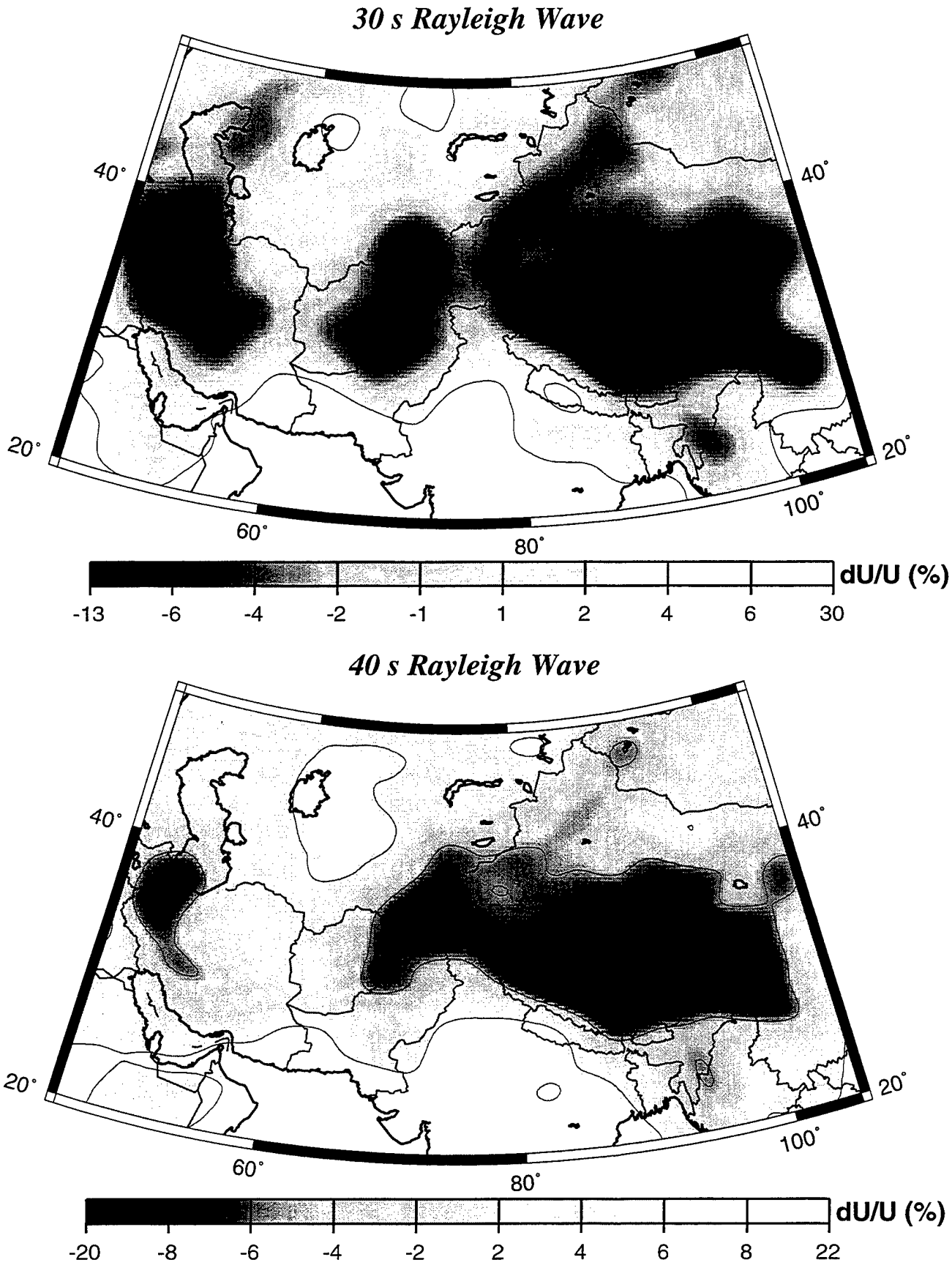

Figure 11c. Same as Figure 11a, but for the 30 s and 40 s Rayleigh waves.

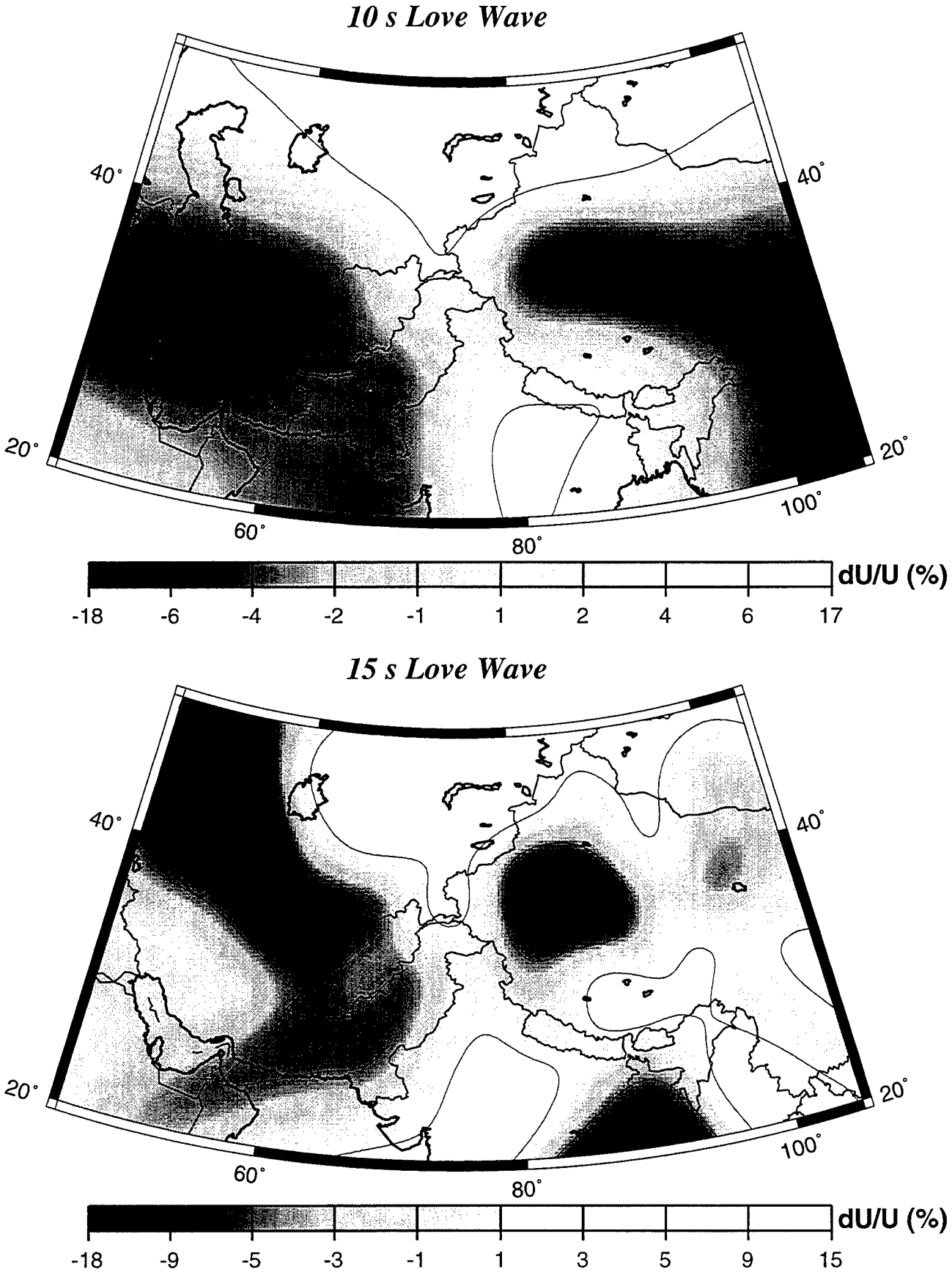

Figure 11d. Same as Figure 11a, but for the 10 s and 15 s Love waves.

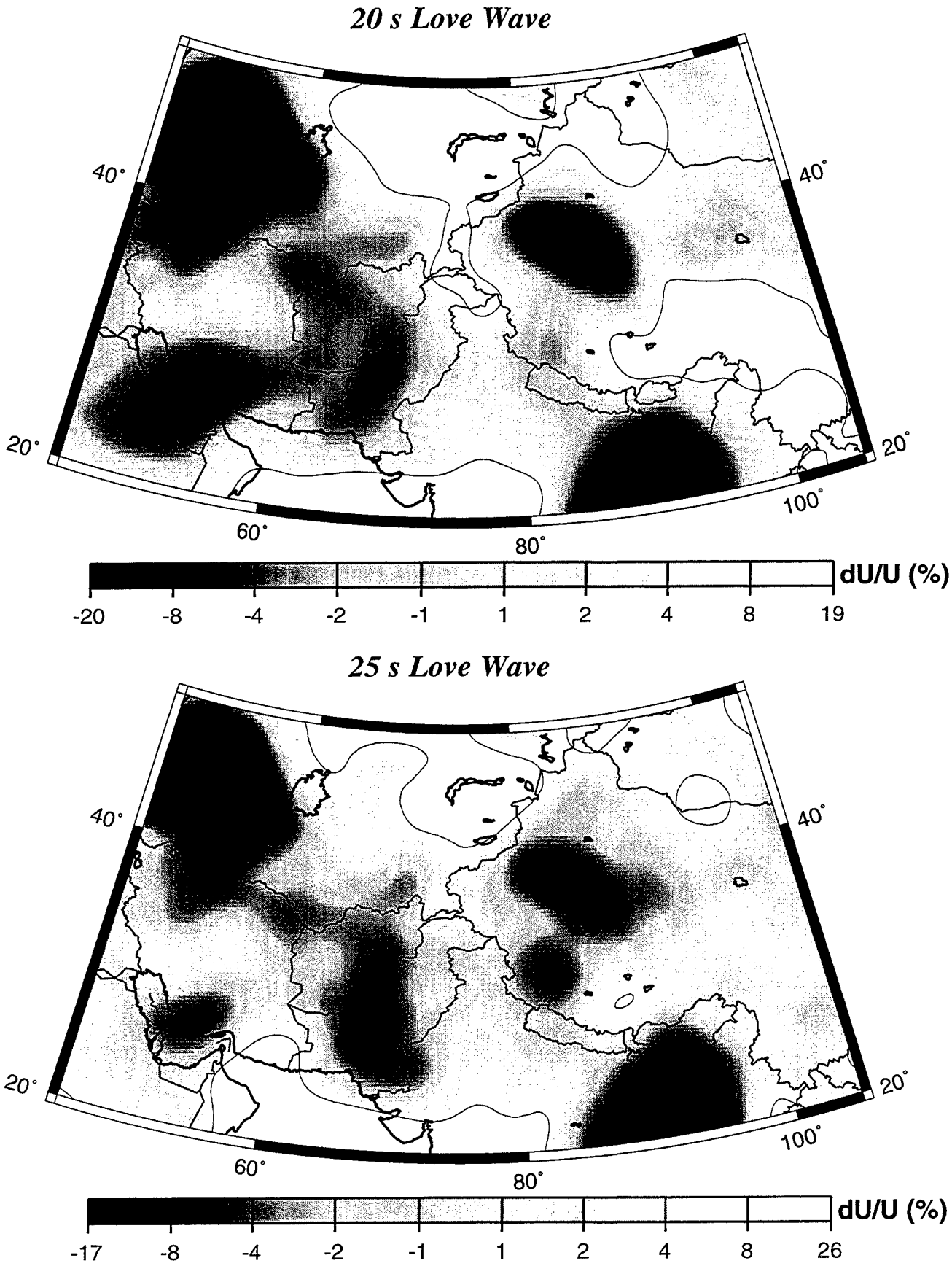

Figure 11e. Same as Figure 11a, but for the 20 s and 25 s Love waves.

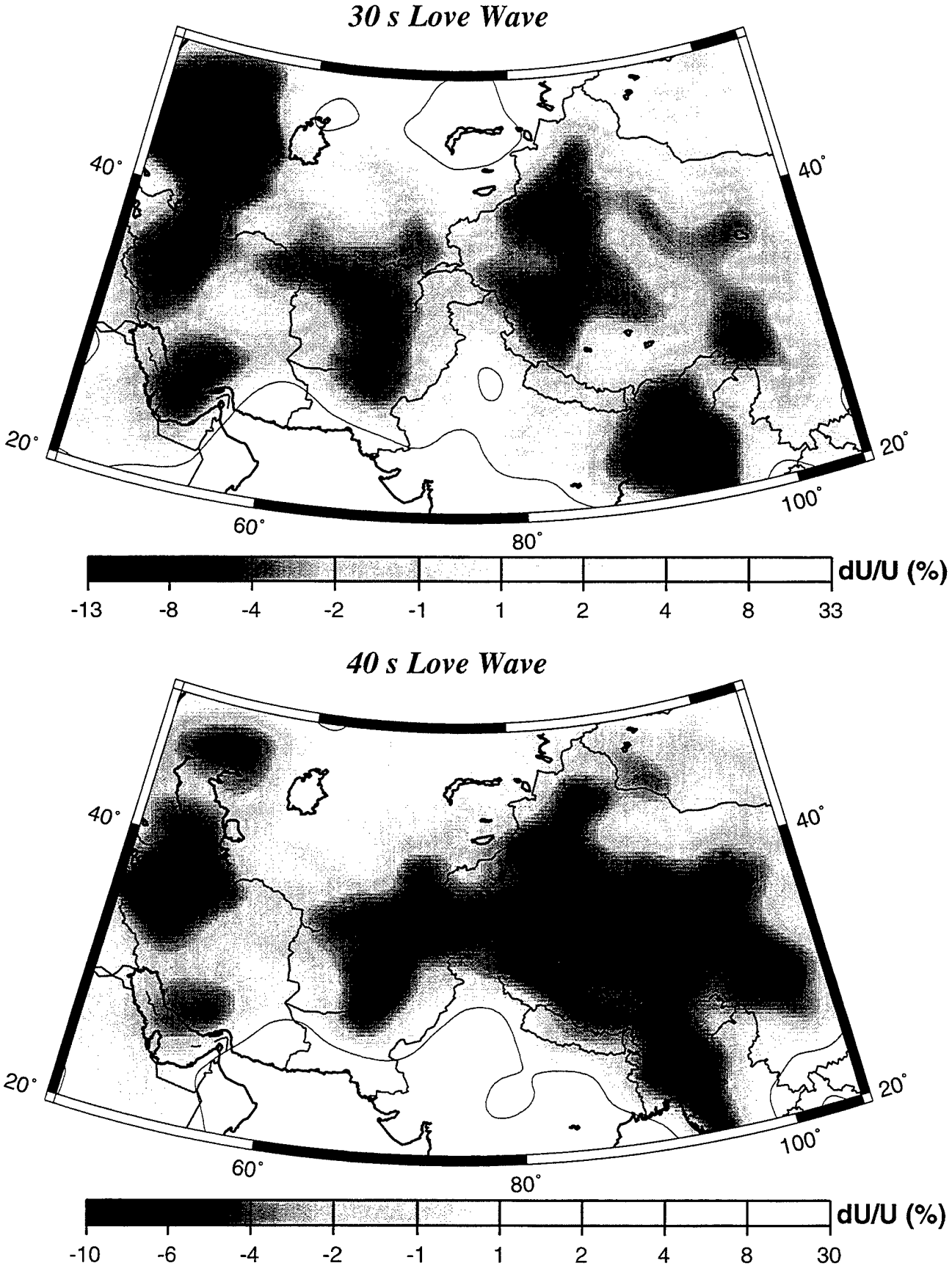

Figure 11f. Same as Figure 11a, but for the 30 s and 40 s Love waves.

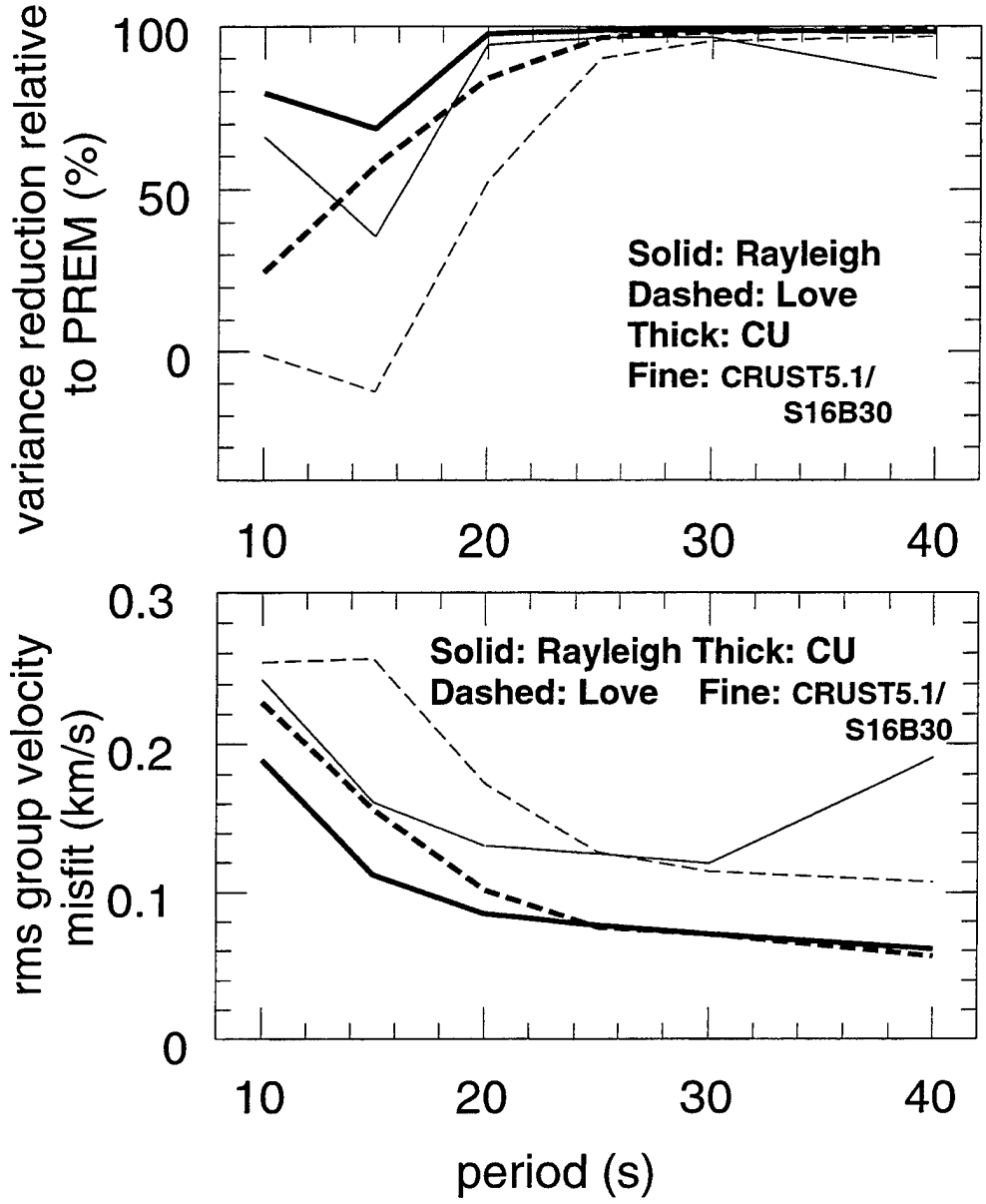

Figure 12. Two measures of misfit to our group velocity measurements for Rayleigh (solid lines) and Love (dashed lines) waves for two different sets of group velocity maps. Thick lines are for our group velocity maps and thin lines are for the group velocity maps predicted by the model composed of the crustal model CRUST-5.1 and the mantle model S16B30.
(Top) Misfit is represented as variance reduction relative to the group velocity from PREM. (Bottom) Misfit is the RMS group velocity misfit [eqn. (5)].

rms group velocity residual:

$$\text{RMS Velocity Misfit} = \left(\frac{1}{N} \sum_i (U_i^{obs} - U_i^{pred})^2 \right)^{1/2}, \quad (5)$$

where N is the number of measurements. For each measure of misfit, comparison is made between the estimated group velocity maps and those predicted by the hybrid model CRUST-5.1/S16B30.

5. Discussion

There have been numerous studies of surface wave dispersion across the studied region within the past 20 years (e.g., Chen and Molnar, 1975; Knopoff and Fouda, 1975; Bird and Toksoz, 1977; Chun and Yoshii, 1977; Patton, 1980; Pines *et al.*, 1980; Knopoff and Chang, 1981; Wier, 1982; Romanowicz, 1982; Feng *et al.*, 1983; Jobert *et al.*, 1985; Brandon and Romanowicz, 1986; Lyon-Caen, 1986; Kozhevnikov and Barmin, 1989; Bourjot and Romanowicz, 1992; Kozhevnikov *et al.*, 1992; Levshin *et al.*, 1992; Wu and Levshin, 1994; Levshin *et al.*, 1994; Levshin and Ritzwoller, 1995; Curtis and Woodhouse, 1996; Ritzwoller *et al.*, 1996b; Zhang, 1996, Griot *et al.*, 1997). Most of these studies have been concentrated on Tibet and have been non-tomographic, multi-station or multi-event phase velocity studies. None of the studies other than our own have resulted in group velocity maps at periods as short as those presented here.

5.1. Qualitative Interpretation of the Group Velocity Maps

Ritzwoller and Levshin (1997) discuss the interpretation of group velocity maps in some detail. However, a number of the features in the group velocity maps shown in Figures 11a - 11f are worthy of further note here. A discussion of the interpretation of these maps should be predicated upon the results of the resolution analysis found in Figures 7a and 7b. These analyses indicate that the 10 s maps are suspect throughout much of the studied region. Indeed, an inspection of the maps in Figures 11a and 11d reveals that very few features have been resolved successfully. The smearing of low and high velocity features toward the edge of the maps is a result of the smoothing in the tomographic inversion. There is very little path coverage near the boundaries of the maps at 10 s period. These maps gives us optimism for

the possibility of the construction of more uniformly accurate and higher resolution maps at 10 s period, but should not yet be interpreted seriously across most of the studied region. At 15 s and above, however, the group velocity signatures of many crustal features begin to emerge clearly, consistent with the results from the resolution analyses.

At the short period end of the study (15 - 25 s), the group velocity maps show the imprint of sedimentary basins and continental platforms and shields. That is, the group velocity maps are dominantly sensitive to shear velocities in the upper crust which are, of course, very slow in sedimentary basins and fast in shield or platform regions. As an example, consider the 20 s Rayleigh and Love wave maps in Figures 11b and 11e. The 20 s Love wave samples somewhat shallower than the Rayleigh wave at the same period. This provides greater sensitivity to sedimentary features, but at this period their sensitivities in continental regions are not substantially different and the maps are seen to be quite similar. Low velocity features are all associated with known sedimentary basins. These include the Tarim Basin, the Ganges Fan and Delta, the Northern and Southern Caspian Depressions, the Persian Gulf, the Tadzhyk Depression (north of Afghanistan and Northern Iran), and a basin associated with the Indus River in Southern Pakistan. These basins provide a characteristic signature on all of the group velocity maps from 15 s - 25 s period. The discrepancies in these features between periods and wave types are attributable to differences in path coverage. For example, the Southern Caspian Depression is not resolved on the 20 s Love wave map but it is on the 20 s Rayleigh wave map. Inspection of the resolution analysis in Figure 5b reveals that the Southern Caspian is not well resolved by the 20 s Love wave and, hence, we have greater confidence in the Rayleigh wave map at this period. Discrepancies such as these should be used to guide future research. Concentrated efforts need to be expended to improve the short period Love wave maps in the Southern Caspian region, as in all regions believed to suffer from relatively poor resolution. High velocity features exist in Central Iran (Iranian Plateau), in Kazakhstan (Kazakh Platform), India (Indian Shield), and Eastern Tibet. A small tongue of high group velocities extends south from the Kazakh Platform to the Pamir (near the Western syntaxis of the Indian-Eurasian plate boundary), which are known to be characterized by very high velocities near the surface.

At the long period end of this study, the group velocities are dominantly sensitive to crustal thickness. This is particularly true for the Rayleigh waves that sample deeper at

each period than the Love waves. Thick crust causes low group velocities. As an example, consider the 40 s Rayleigh and Love wave maps in Figures 11c and 11f. By 40 s period, both types of waves possess considerable sensitivity to Moho depth, although the Love wave continues to have substantial sensitivity to upper crustal and sedimentary velocities. The effects of crustal thickness on the estimated group velocity maps are most striking under Tibet where the Moho extends to depths greater than 70 km. Low velocity anomalies are associated with Tibet, the Pamir and the Hindu Kush, the Altai Range in Mongolia, and the Zagros Mountains in Western Iran. The 40 s Love wave map continues to be imprinted with low velocities associated with the deepest basins; e.g., the Tarim, the Caspian, and the Ganges.

In summary, a qualitative inspection of the group velocity maps in Figures 11a - 11f reveals that:

- the observed group velocity features are repeatable in that similar features are observed at different periods and wave types which sample the Earth similarly;
- these repeatable features are qualitatively understandable in terms of known geological and tectonic structures, particularly sedimentary basins, continental platforms and shields, and crustal thicknesses;
- discrepancies that exist between the maps are understandable in terms of differences in path coverage;
- the features observed on the group velocity maps at 20 s period differ substantially from those observed at 40 s period since different crustal structures dominate the maps at these two periods.

The final comment indicates that it would be a mistake to use group velocity maps constructed around 40 s period and attempt to extrapolate them for use at much shorter periods. This is particularly true in Central Asia which is characterized by extremely thick crust and deep sedimentary basins.

5.2. Comparison with the Model CRUST-5.1/S16B30

In comparing the observed maps with predictions from CRUST-5.1/S16B30 several comments are in order. First, CRUST-5.1 is principally a v_p model in which the v_s variations have been approximated by use of a realistic Poisson's Ratio, and much of the crust in the studied region is relatively unconstrained by seismological data at the disposal of Mooney *et al.*. Second, CRUST-5.1 is defined on a 5 degree grid in which velocities are assumed constant within each cell. A number of discrepancies between the observed and predicted maps result from differences in resolution. Finally, only the crustal part of CRUST-5.1/S16B30 appreciably affects group velocities across the continental parts of the studied region. Thus, we are only testing CRUST-5.1 at the periods of this study.

Figures 13a and 13b present group velocity maps predicted from the model CRUST-5.1/S16B30 at 20 s and 40 s period. Since CRUST-5.1 is defined on a 5° grid, group velocity maps are characterized by square blocks possessing approximately constant velocities. The imprint of sedimentary depressions in CRUST-5.1 is clearly present on the 20 s maps. In particular, the Northern and Southern Caspian Depressions, the Persian Gulf, and the Ganges Fan and Delta are apparent and are particularly strong for the Love wave. At 40 s, the signature of crustal thickness emerges, with Tibet most strongly imprinting the 40 s Rayleigh wave map. These predictions are qualitatively in good agreement with many aspects of the observed maps in Figures 11b, 11c, 11e, and 11f. There are the following discrepancies, however. (1) CRUST-5.1 misses some of the smaller sedimentary depressions such as the Tarim Basin and the Tadzhyk Depression. (2) Predicted group velocity anomalies caused by sedimentary basins are typically too low and continue on maps to longer periods than observed. This indicates that the sedimentary velocities in deep basins may be too slow in the model. (3) CRUST-5.1 also misses some of the smaller mountain ranges such as the Zagros and the Altai Ranges which are clearly observed in the 40 s Rayleigh wave map. (4) The geometry of crustal thickening associated with Tibet, the Himalaya, the Pamir, the Hindu Kush, the Tien Shan, and the Altai Ranges cannot be well represented by a 5° gridded model.

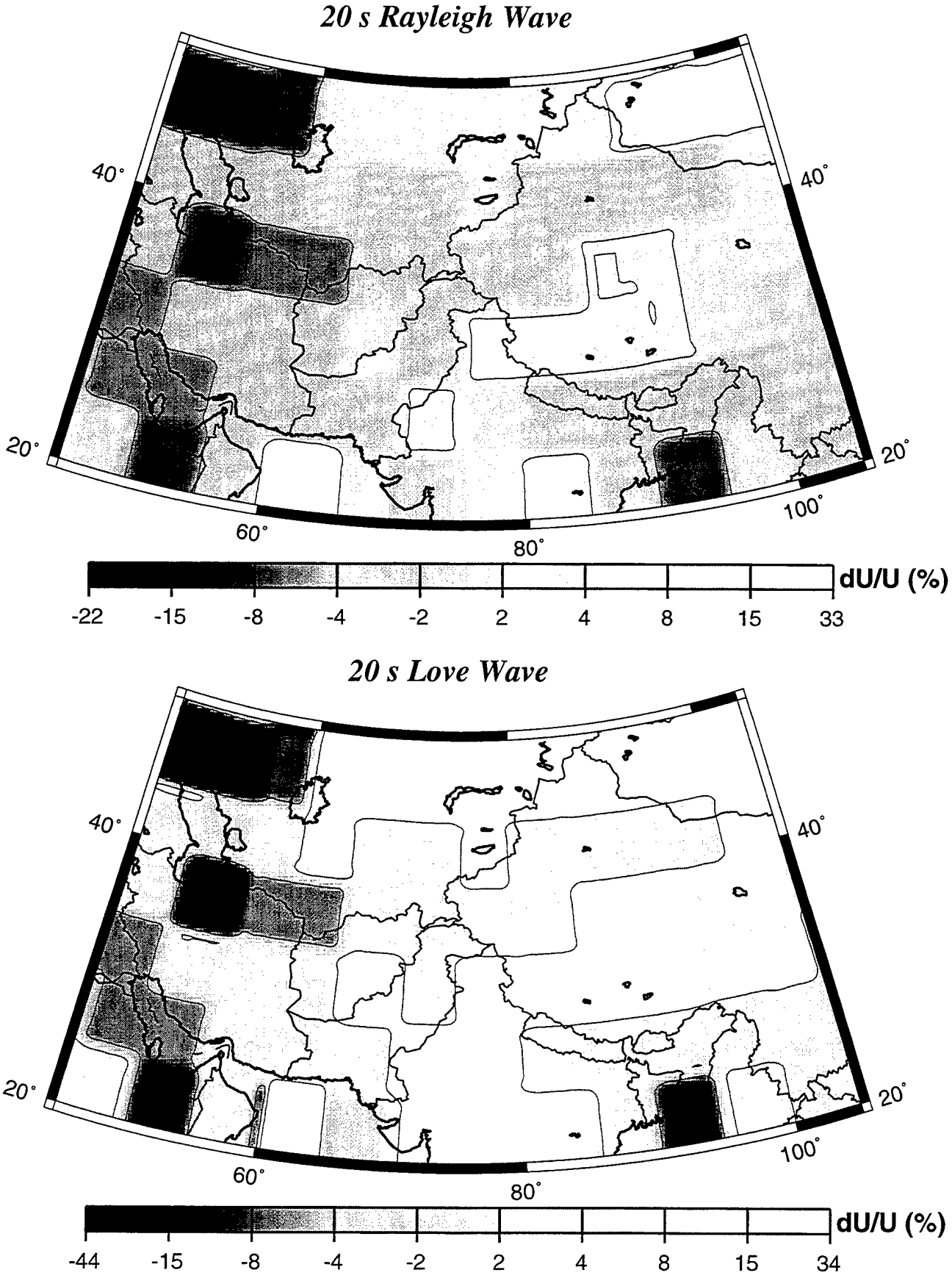

Figure 13a. Group velocity maps across the region of study for the 20 s Rayleigh and Love waves predicted by the model CRUST-5.1/S16B30.

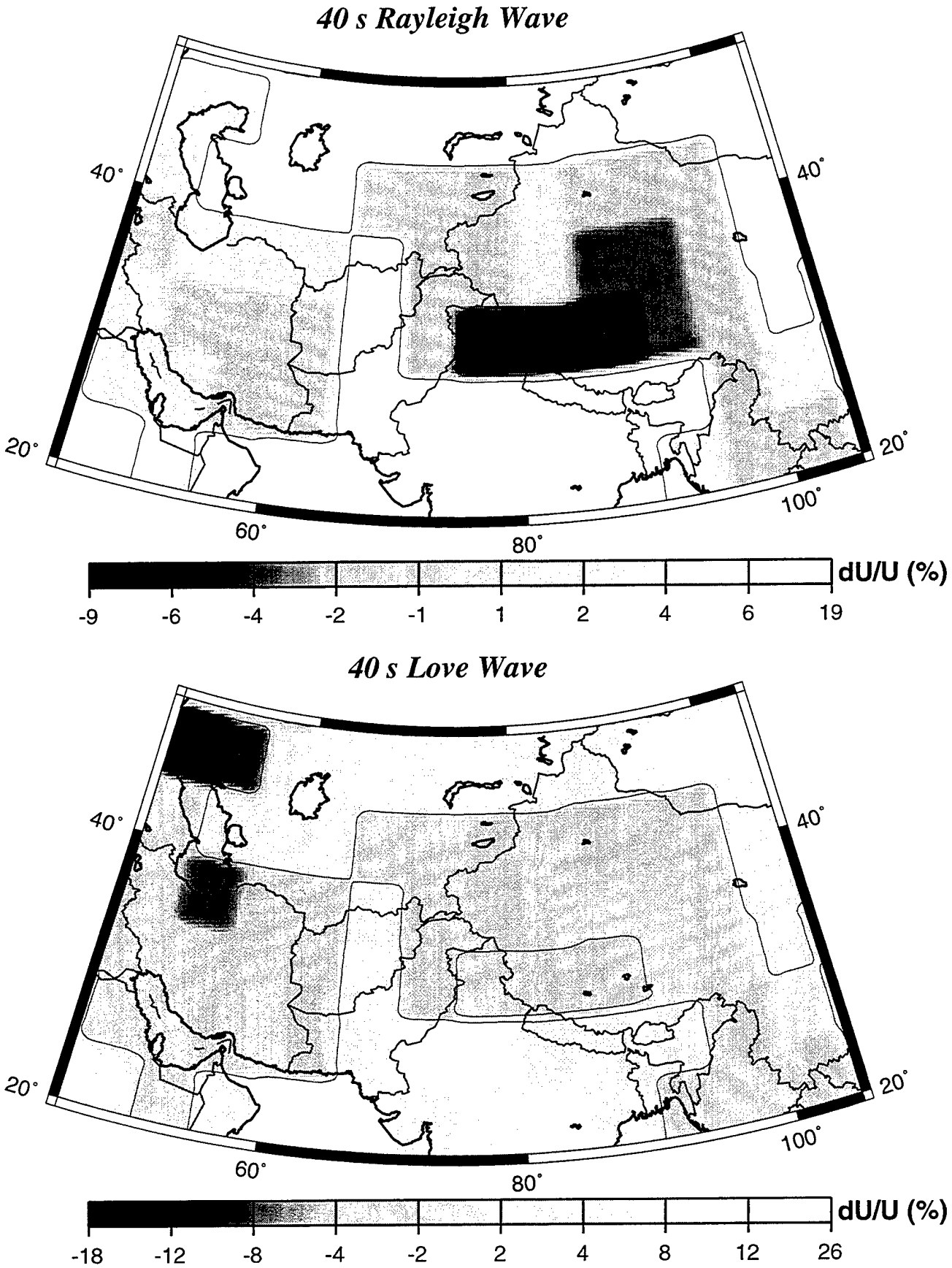

Figure 13b. Same as Figure 13a, but for the 40 s Rayleigh and Love waves.

5.3. Misfit

As discussed directly above, the group velocity maps predicted by CRUST-5.1 are qualitatively in good agreement with the observed maps. However, sedimentary velocities appear to be too low in CRUST-5.1 and there are significant features observed which are smaller in scale than those representable by a 5° gridded model. The question we ask here is, what is the effect of these observed differences on the fit to the group velocity observations? This question is addressed by Figure 13 which presents the variance reduction and rms group velocity misfit between the observed group velocity curves and those predicted by our maps and the group velocity maps predicted by CRUST-5.1/S16B30. These measures of misfit are applied to all measurements whose paths at least touch the studied region.

Variance reductions to the observed group velocity measurements provided by CRUST-5.1/S16B30 are large and positive for Rayleigh waves at 15 s and above and for Love waves at 20 s and above. Indeed, variance reductions are in excess of 80% for Rayleigh waves between 20 and 40 s period and for Love waves between 25 and 40 s. The degradation in misfit of CRUST-5.1/S16B30 at shorter periods is partially due to the fact that several sedimentary basins are missing in the model, as discussed above. As discussed further below, however, measurement uncertainties and off-pure-path propagation also increase at short periods and these factors contribute to increase the misfit of both the observed and the model group velocity maps below 25 s period. The slight degradation in variance reduction for the 40 s Rayleigh wave is due to errors in crustal thickness in CRUST-5.1. This is more clearly observed as a substantial increase in rms-misfit for the 40 s Rayleigh wave. The variance reduction degrades more subtly than the rms-misfit since signal levels due to crustal thickness variations increase along with the misfit.

Problems in CRUST-5.1 associated with modeling sedimentary basins and crustal thicknesses strongly imprint the data in this period range. Thus, the observed maps fit the group velocity measurements substantially better than the predictions from CRUST-5.1/S16B30, particularly for Love waves below 20 s period due to their very strong sensitivity to sedimentary basins and for Rayleigh waves at 40 s period due to their sensitivity to crustal thickness. Variance reductions of the observed maps relative to PREM are in excess of 90% at 20 s and longer periods for Rayleigh waves and at 25 s and higher for Love waves. At 25 s and beyond, the rms-misfits for Rayleigh and Love waves are nearly equal and lie between

0.06 - 0.07 km/s, on average about one-half of the misfit of CRUST-5.1/S16B30. Below 20 s period misfit rises rapidly, but remains about one-half that of CRUST-5.1/S16B30. This rise is caused by two factors. First, measurements are harder to make accurately below 20 s period due to scattering. The analyst has a harder time constructing a frequency-time filter which reliably separates directly arriving surface waves from coda. Comparison of Figures 2b and 13 indicates that misfit is about twice the estimated standard deviation independent of period. Thus, about one-half of misfit results from observational errors. Second, off-pure-path propagation becomes extremely important in this period range (e.g., Levshin *et al.*, 1994). This phenomenon and event mislocation are the likely causes of the remainder of misfit.

These observations allow us to conclude that the observed maps should prove superior in predicting group arrival times and should prove useful in calibrating crustal models such as CRUST-5.1. However, improvements at periods below 20 s period are still needed. In particular, the incorporation of off-pure-path propagation at these periods may be necessary to provide better fits to the data. In addition, the resolution analyses indicate that there are parts of the studied region which remain poorly constrained at all periods.

6. Conclusions

We have reported the results of a systematic study of intermediate period (10 s - 40 s) Rayleigh and Love wave dispersion across Central Asia, Western China, and parts of the Middle East. There are three main reasons why we believe that this study represents a significant improvement in the understanding of intermediate period surface wave dispersion across the studied region. The first has to do with the data used. This study displays denser and more uniform data coverage and demonstrates higher resolution than previous studies that have been performed on this scale and at these periods. Second, the group velocity maps display the signatures of known geological and tectonic features never before revealed in surface wave studies on this scale. In particular, these maps are providing entirely new constraints on sedimentary basins and crustal thicknesses. This both lends credence to the maps and spurs interest in their use to infer information about the features that are observed. Finally, the group velocity maps provide a significant improvement in fit to the observed dispersion curves. For these reasons we believe that the group velocity maps presented here

should prove useful to predict group travel times for the identification and extraction of surface wave packets, to calibrate existing crustal models such as CRUST-5.1, and as data in inversions for crustal models (e.g., Ritzwoller *et al.*, 1996a).

There are several keys elements to estimating group velocity maps at these periods. First, regional earthquakes need to occur and there must be broadband instrumentation in the region of study. Second, dispersion measurements must be performed carefully to separate the first arrival from coda and other interfering waves. Third, data from smaller earthquakes than those normally studied on continental or global scales need to be processed (i.e., $M_s \leq 5.0$). Finally, the regional measurements should be combined with measurements made on a larger spatial scale. The inclusion of measurements on paths that propagate more broadly across Eurasia provides greater homogeneity of coverage and azimuthal distribution across the studied region and appreciably improves resolution and accuracy.

The methods described here can continue to be applied across the studied region and more generally across Eurasia to new and accumulating data in order to improve resolution and reliability further. In fact, this study is far from complete even across the studied region. For example, we have only analyzed data from small events ($M_s \leq 5.0$) at KNET and KAZNET. The analysis of data from GSN, CDSN, GEOSCOPE, and PASSCAL installations across the studied region could improve path coverage substantially, particularly below 20 s period where the path coverage is most inhomogeneous. Substantial improvements can still be achieved in the most poorly resolved parts of the studied region; e.g., Northwestern Iran, India, etc.. The methods can also be applied successfully to other areas across Eurasia and to selected regions on other continents. In particular, improvements in instrumentation in the Middle East (e.g., Vernon *et al.*, 1996) and the Far East identify regions of promise for future application of these methods.

There remain several shortcomings with the methodology of this study that point the way for future technical enhancements. Most significantly, the use of phase information would help provide tighter constraints on crustal structures. In addition, off-great-circle propagation is significant at the periods studied here. Modeling it by ray tracing through phase velocity maps and potentially using polarization information are also obvious directions for the future.

7. Recommendations

We have presented in this report the results of a study of the dispersion characteristics of intermediate period fundamental surface waves propagating across Central Asia, Western China, and parts of the Middle East. This study displays denser and more uniform data coverage and demonstrates higher resolution ($\sim 4°$) than previous studies that have been performed on this scale and at these periods. The main outcome of this study are the group velocity maps from 10 s to 40 s period for both Rayleigh and Love waves and the resolution analyses that aim to guide the use of these maps. These group velocity maps display the signatures of known geological and tectonic features never before revealed in surface wave studies on this scale, and provide a significant improvement in fit to the observed dispersion curves. Still, the achieved resolution is not uniform across the region of study, and may be significantly improved by acquiring and processing additional data from global and regional networks, as well as temporary PASSCAL deployments.

High resolution group velocity maps of this kind are needed to improve the ability to detect surface wave packets with periods at and less than 20 s, to make accurate spectral amplitude measurements on the extracted wave forms, and, thereby, to apply the classical $M_s : m_b$ discriminant, or other discriminants based in part on surface wave amplitudes, to small regional events. More accurate crustal shear velocity models obtained as a result of the inversion of such maps should help to develop improved methods of location and depth estimation, to improve understanding of surface wave wave propagation across the region of study, and to permit more accurate synthetic wavefield simulations. To meet these goals, we make the following recommendations.

- The use of estimated maps in developing matched filter techniques to detect and extract surface wave signals at and below 20 s period generated by relatively weak shallow events inside the studied region.

- The more general application of the methodology developed in our research to the detailed study of intermediate period surface wave propagation in strategically important seismically active regions across Eurasia - in particular the Middle East, Central and Southern Asia, and the Far East. High resolution group velocity maps, such as those we present here centered on Central Asia, can and should be constructed in the Middle

and Far East and significant improvements in Central Asia remain possible.

- The construction of more accurate crustal and lithospheric shear velocity models using the estimated (and continually improving) group velocity maps.

References

Bird, P. and M.N. Toksoz, Strong attenuation of Rayleigh waves in Tibet, *Nature*, **266**, 161 - 163, 1977.

Bourjot, L. and B. Romanowicz, Crust and upper mantle tomography in Tibet using surface waves, *Geophys. Res. Let.*, **19**, 1992.

Brandon, C. and B. Romanowicz, A 'no-lid' zone in the Central Chang-Thang platform of Tibet: Evidence from pure path phase velocity measurements of long period Rayleigh waves, *J. Geophys. Res.*, **91**, 6547 - 6564, 1986.

Chen, W.-P. and P. Molnar, Short-period Rayleigh wave dispersion across the Tibetan Plateau, *Bull. Seism. soc. Amer.*, **65**, 1051 - 1057, 1975.

Chun, K.Y. and T. Yoshii, Crustal structure of the Tibetan Plateau: a surface wave study, *Bull. Seism. soc. Amer.*, **67**, 735 - 750, 1977.

Curtis, A. and R. Snieder, Surface wave phase velocities and shear velocity structure beneath Eurasia, to be submitted to *J. Geophys. Res.*, 1997.

Curtis, A. and J. Woodhouse, Crust and upper mantle shear velocity structure beneath the Tibetan plateau and surrounding regions from inter-event surface wave phase velocity inversion, submitted to *Geophys. J. Int.*, 1996.

Das, T. and G. Nolet, Crustal thickness using high frequency Rayleigh waves, *Geophys. Res. Lett.*, **22**, 539 - 542, 1995.

Ditmar, P.G., and Yanovskaya, T.B., A generalization of the Backus-Gilbert method for estimation of lateral variations of surface wave velocity, *Izv. AN SSSR, Fizika Zemli (Solid Earth)*, **6**, 30 - 60, 1987. (Russian original).

Dziewonski, A. M. and D. L. Anderson, Preliminary Reference Earth Model, *Phys. Earth Planet. Int.*, **25**, 297-356, 1981.

Dziewonski, A.M., T.-A. Chou, and J.H. Woodhouse, Determination of earthquake source parameters from waveform data for studies of global and regional seismicity, *J. Geophys. Res.*, **86**, 2825 - 2852, 1981.

Ekstrom, G., J. Tromp, and E.W.F. Larson, Measurements and global models of surface wave propagation, *J. Geophys. Res.*, **102**, 8147 - 8158, 1997.

Feng, C.C. and T. Teng, Three-dimensional crust and upper mantle structure of the Eurasian continent, *J. Geophys. Res.*,**88**, 2261 - 2272, 1983.

Feng, R., J.S. Zhu, Y. Y. Ding, G.Y. Chen, Z. Q. He, S. B. Yang, H. N. Zhou, and K. Z. Sun, Crustal structure in China from surface waves, in: *Chinese Geophysics*, Am. Geophys. Union, **2**, 273-289, 1983.

Griot, D.A., J.P. Montagner, and P. Tapponier, Surface wave phase velocity tomography and azimuthal anisotropy in Central Asia, submitted to *J. Geophys. Res.*, 1997.

Jobert, N., B. Journet, G. Jobert, A. Hirn, and S.-K. Zhong, Deep structure of southern Tibet inferred from the dispersion of Rayleigh waves through a long-period seismic network, *Nature*, **313**, 386 - 388, 1985.

Kim, W-Y., V. V. Kazakov, A. G. Vanchugov, and D. W. Simpson, Broadband and array observations at low noise sites in Kazakhstan: Opportunities for seismic monitoring of a Comprehensive Test Ban Treaty. In *Monitoring a Comprehensive Test Ban Treaty*, (editors E. S.Husebye), 1995.

Knopoff, L and F.-S. Chang, Upper mantle structure under the Tibetan Plateau, in *Geological and Ecological Studies of the Qinghai-Xizang Plateau*, **1**, 627 - 632, ed. Liu Dong-Sheng, Gordon and Breach, New York, 1981.

Knopoff, L and A.A. Fouda, Upper mantle structure under the Arabian Peninsula, *Tectonophys.*, **26**, 121 - 134, 1975.

Knopoff, L. and F.A. Schwab, Apparent initial phase of a source of Rayleigh waves, *J. Geophys. Res.*, **73**, 755 - 760, 1968.

Kozhevnikov, V. M., and M. P. Barmin, Dispersion curves of Rayleigh wave group velocities for several regions of the Asian continent. *Izv. AN SSSR, Fizika Zemli (Solid Earth)*, no. 9, 16-25, 1989.

Kozhevnikov, V. M., D. E. Lokshtanov, and M. P. Barmin, Shear-velocity structure of the lithosphere for nine large tectonic regions of the Asian continent. *Izv. AN SSSR, Fizika*

Zemli (Solid Earth), no. 1, 61-70, 1992.

Laske, G. and G. Masters, Constraints on global phase velocity maps from long-period polarization data, *J. Geophys. Res.*, **101**, 16,059 - 16,075, 1996.

Levshin, A. L., Pisarenko, V. F., and G. A. Pogrebinsky, On a frequency-time analysis of oscillations, *Ann. Geophys.*, **28**, 211 - 218, 1972.

Levshin, A. L., T. B. Yanovskaya, A. V. Lander, B. G. Bukchin, M. P. Barmin, L. I. Ratnikova, and E. N. Its, *Seismic surface waves in a laterally inhomogeneous Earth*, (ed. V. I. Keilis-Borok), Kluwer Publ., Dordrecht, 1989.

Levshin, A. L., L. Ratnikova, and J. Berger, Peculiarities of surface wave propagation across Central Eurasia, *Bull. seism. Soc. Am.*, **82**, 2464 - 2493, 1992.

Levshin, A. L., M. H. Ritzwoller, and L. I. Ratnikova, The nature and cause of polarization anomalies of surface waves crossing northern and central Eurasia, *Geophys. J. Int.*, **117**, 577 - 590, 1994.

Levshin, A.L. and M. H. Ritzwoller, Characteristics of surface waves generated by events on and near the Chinese nuclear test site, *Geophys. J. Int.*, **123**, 131-149, 1995.

Levshin, A.L., M.H. Ritzwoller, and J.S. Resovsky, The effect of source phase on group travel times and group velocity maps, to be submitted to *Geophys. J. Int.*, Spring, 1997.

Lyon-Caen, H., Comparison of the upper mantle shear wave velocity structure of the Indian Shield and the Tibetan Plateau and tectonic implications, *Geophys. J. R. astron. Soc.*, **86**, 727 - 749, 1986.

Masters, G., S. Johnson, G. Laske, and H. Bolton, A shear-velocity model of the mantle, *Phil. Trans. R. Soc. Lond. A*, **354**, 1385-1411, 1996.

Montagner, J.P. and T. Tanimoto, Global upper mantle tomography of seismic velocities and anisotropies, *J. Geophys. Res.*, **96**, 20337 - 20351, 1991.

Mooney, W.D., G. Laske, and G. Masters, CRUST 5.1: A global crustal model at 5 degrees by 5 degrees, submitted to *J. Geophys. Res.*, 1996.

Patton, H., Crustal and upper mantle structure of the Eurasian continent from the phase

velocity and Q of surface waves. *J. Rev. Geophys. Space Phys.*, **18**, 605-625, 1980.

Pavlis G., H. Al-Shukri, H. Mahdi, and D. Repin, JSP arrays and networks in Central Asia, *IRIS Newsletter*, **XIII**, **2**, 10-12, 1994.

Pines, I., T.-L. Teng, and R. Rosenthal, A surface wave dispersion study of the crustal and upper mantle structure of China, *J. Geophys. Res.*, **85**, 3829 - 3844, 1980.

Quinlan, D.M., Datascope: A relational database system for scientists, *EOS Trans. Am. Geophys. Union.*, **75**, F431, 1994.

Ritzwoller, M.H., A.L. Levshin, S.S. Smith, and C.S. Lee, Making accurate continental broadband surface wave measurements, *Proceedings of the 17th Seismic Research Symposium on Monitoring a CTBT*, 482-490, 1995, PL-TR-95-2108, ADA310037.

Ritzwoller, M.H., A.L. Levshin, and L.I. Ratnikova, Surface wave tomography across Tibet, *EOS Trans. Am. Geophys. Un.*, **77**, F675, 1996a.

Ritzwoller, M.H., A.L. Levshin, L.I. Ratnikova, and D.M. Tremblay, High resolution group velocity variations across Central Asia, *Proceedings of the 18th Seismic Research Symposium on Monitoring a CTBT*, 98 - 107, 1996b, PL-TR-96-2153, ADA313692.

Ritzwoller, M.H. and A.L. Levshin, Eurasian surface wave tomography: Group velocities, submitted to *J. Geophys. Res.*, 1997.

Romanowicz, B.A., Constraints on the structure of the Tibet Plateau from pure-path phase velocities of Love and Rayleigh waves, *J. Geophys. Res.*, **87**, 6865 - 6883, 1982.

Russell, D. W., R. B. Herrman, and H. Hwang, Application of frequency-variable filters to surface wave amplitude analysis, *Bull. seism. Soc. Am.*, **78**, 339 - 354, 1988.

Stevens, J.L. and S.M. Day, The physical basis for m_b : M_s and variable frequency magnitude methods for earthquake/explosion discrimination, *J. Geophys. Res.*, **90**, 3009 - 3020, 1985.

Trampert, J. and J. Woodhouse, Global phase velocity maps of Love and Rayleigh waves between 40 and 150 seconds, *Geophys. J. Int.*, **122**, 675 - 690, 1995.

Vernon, F., The Kyrghyz Seismic Network, *IRIS Newsletter*, **XIII**, 7-8, 1994.

Vernon, F., Mellors, R.J., J. Berger, A.M. Al-Amri, J. Zollweg, Initial results from the deploy-

ment of broadband seismometers in the Saudi Arabian Shield, *Proceedings of the 18th Seismic Research Symposium on Monitoring a CTBT*, 108 - 117, 1996, PL-TR-96-2153, ADA313692.

Wessel, P., and W.H. F. Smith, New version of the Generic Mapping Tools released, *EOS Trans. AGU*, **76**, 329, 1995.

Wessel, P., and W.H. F. Smith, 1991, Free software helps map and display data, *EOS Trans. AGU*, **72**, 441, 1991.

Wier, S., Surface wave dispersion and Earth structure in South-Eastern China, *Geophys. J. Roy. Astr. Soc.*, **69**, 33-47, 1982.

Wu, F.T. and A. Levshin, Surface wave group velocity tomography of East Asia, *Phys. Earth Planet. Int.*, **84**, 59 - 77, 1994.

Yanovskaya, T.B., and P.G. Ditmar, Smoothness criteria in surface wave tomography. *Geophys. J. Int.*, **102**, 63-72, 1990.

Zhang, Y.-S., Three-dimensional velocity structure beneath East Asia and its tectonic implication, submitted to *Mantle Dynamics and Plate Interactions in East Asia*, AGU/GSA Geodynamics Series, 1996.

THOMAS AHRENS
SEISMOLOGICAL LABORATORY 252-21
CALIFORNIA INSTITUTE OF TECHNOLOGY
PASADENA, CA 91125

SHELTON ALEXANDER
PENNSYLVANIA STATE UNIVERSITY
DEPARTMENT OF GEOSCIENCES
537 DEIKE BUILDING
UNIVERSITY PARK, PA 16801

T.G. BARKER
MAXWELL TECHNOLOGIES
8888 BALBOA AVE.
SAN DIEGO, CA 92123-1506

THERON J. BENNETT
MAXWELL TECHNOLOGIES
11800 SUNRISE VALLEY DRIVE SUITE 1212
RESTON, VA 22091

JONATHAN BERGER
UNIVERSITY OF CA, SAN DIEGO
SCRIPPS INSTITUTION OF OCEANOGRAPHY IGPP, 0225
9500 GILMAN DRIVE
LA JOLLA, CA 92093-0225

STEVEN BRATT
NTPO
1901 N. MOORE STREET, SUITE 609
ARLINGTON, VA 22209

LESLIE A. CASEY
DOE
1000 INDEPENDENCE AVE. SW
NN-20
WASHINGTON, DC 20585-0420

STANLEY DICKINSON
AFOSR
110 DUNCAN AVENUE, SUITE B115
BOLLING AFB
WASHINGTON, D.C. 20332-001

RICHARD J. FANTEL
BUREAU OF MINES
DEPT OF INTERIOR, BLDG 20
DENVER FEDERAL CENTER
DENVER, CO 80225

ROBERT GEIL
DOE
PALAIS DES NATIONS, RM D615
GENEVA 10, SWITZERLAND

RALPH ALEWINE
NTPO
1901 N. MOORE STREET, SUITE 609
ARLINGTON, VA 22209

MUAWIA BARAZANGI
INSTITUTE FOR THE STUDY OF THE CONTINENTS
3126 SNEE HALL
CORNELL UNIVERSITY
ITHACA, NY 14853

DOUGLAS BAUMGARDT
ENSCO INC.
5400 PORT ROYAL ROAD
SPRINGFIELD, VA 22151

WILLIAM BENSON
NAS/COS
ROOM HA372
2001 WISCONSIN AVE. NW
WASHINGTON, DC 20007

ROBERT BLANDFORD
AFTAC
1300 N. 17TH STREET
SUITE 1450
ARLINGTON, VA 22209-2308

RHETT BUTLER
IRIS
1200 NEW YORK AVE., NW
SUITE 800
WASHINGTON, DC 20005

CATHERINE DE GROOT-HEDLIN
UNIVERSITY OF CALIFORNIA, SAN DIEGO
INSTITUTE OF GEOPHYSICS AND PLANETARY PHYSICS
8604 LA JOLLA SHORES DRIVE
SAN DIEGO, CA 92093

DIANE I. DOSER
DEPARTMENT OF GEOLOGICAL SCIENCES
THE UNIVERSITY OF TEXAS AT EL PASO
EL PASO, TX 79968

MARK D. FISK
MISSION RESEARCH CORPORATION
735 STATE STREET
P.O. DRAWER 719
SANTA BARBARA, CA 93102-0719

LORI GRANT
MULTIMAX, INC.
311C FOREST AVE. SUITE 3
PACIFIC GROVE, CA 93950

HENRY GRAY
SMU STATISTICS DEPARTMENT
P.O. BOX 750302
DALLAS, TX 75275-0302

DAVID HARKRIDER
PHILLIPS LABORATORY
EARTH SCIENCES DIVISION
29 RANDOLPH ROAD
HANSCOM AFB, MA 01731-3010

THOMAS HEARN
NEW MEXICO STATE UNIVERSITY
DEPARTMENT OF PHYSICS
LAS CRUCES, NM 88003

DONALD HELMBERGER
CALIFORNIA INSTITUTE OF TECHNOLOGY
DIVISION OF GEOLOGICAL & PLANETARY SCIENCES
SEISMOLOGICAL LABORATORY
PASADENA, CA 91125

ROBERT HERRMANN
ST. LOUIS UNIVERSITY
DEPARTMENT OF EARTH & ATMOSPHERIC SCIENCES
3507 LACLEDE AVENUE
ST. LOUIS, MO 63103

ANTHONY IANNACCHIONE
BUREAU OF MINES
COCHRANE MILL ROAD
PO BOX 18070
PITTSBURGH, PA 15236-9986

THOMAS JORDAN
MASSACHUSETTS INSTITUTE OF TECHNOLOGY
EARTH, ATMOSPHERIC & PLANETARY SCIENCES
77 MASSACHUSETTS AVENUE, 54-918
CAMBRIDGE, MA 02139

LAWRENCE LIVERMORE NATIONAL LABORATORY
ATTN: TECHNICAL STAFF (PLS ROUTE)
PO BOX 808, MS L-221
LIVERMORE, CA 94551

LAWRENCE LIVERMORE NATIONAL LABORATORY
ATTN: TECHNICAL STAFF (PLS ROUTE)
PO BOX 808, MS L-208
LIVERMORE, CA 94551

LAWRENCE LIVERMORE NATIONAL LABORATORY
ATTN: TECHNICAL STAFF (PLS ROUTE)
PO BOX 808, MS L-195
LIVERMORE, CA 94551

I. N. GUPTA
MULTIMAX, INC.
1441 MCCORMICK DRIVE
LARGO, MD 20774

IAN MACGREGOR
NSF
4201 WILSON BLVD., ROOM 785
ARLINGTON, VA 22230

MICHAEL HEDLIN
UNIVERSITY OF CALIFORNIA, SAN DIEGO
SCRIPPS INSTITUTION OF OCEANOGRAPHY IGPP, 0225
9500 GILMAN DRIVE
LA JOLLA, CA 92093-0225

EUGENE HERRIN
SOUTHERN METHODIST UNIVERSITY
DEPARTMENT OF GEOLOGICAL SCIENCES
DALLAS, TX 75275-0395

VINDELL HSU
HQ/AFTAC/TTR
1030 S. HIGHWAY A1A
PATRICK AFB, FL 32925-3002

RONG-SONG JIH
HQ DSWA/PMP/CTBT
6801 TELEGRAPH ROAD
ALEXANDRIA, VA 22310-3398

LAWRENCE LIVERMORE NATIONAL LABORATORY
ATTN: TECHNICAL STAFF (PLS ROUTE)
PO BOX 808, MS L-200
LIVERMORE, CA 94551

LAWRENCE LIVERMORE NATIONAL LABORATORY
ATTN: TECHNICAL STAFF (PLS ROUTE)
LLNL
PO BOX 808, MS L-175
LIVERMORE, CA 94551

LAWRENCE LIVERMORE NATIONAL LABORATORY
ATTN: TECHNICAL STAFF (PLS ROUTE)
PO BOX 808, MS L-202
LIVERMORE, CA 94551

LAWRENCE LIVERMORE NATIONAL LABORATORY
ATTN: TECHNICAL STAFF (PLS ROUTE)
PO BOX 808, MS L-205
LIVERMORE, CA 94551

THORNE LAY
UNIVERSITY OF CALIFORNIA, SANTA CRUZ
EARTH SCIENCES DEPARTMENT
EARTH & MARINE SCIENCE BUILDING
SANTA CRUZ, CA 95064

ATTN: LIBRARIAN
CENTER FOR MONITORING RESEARCH
1300 N. 17th STREET, SUITE 1450
ARLINGTON, VA 22209

LOS ALAMOS NATIONAL LABORATORY
ATTN: TECHNICAL STAFF (PLS ROUTE)
PO BOX 1663, MS F659
LOS ALAMOS, NM 87545

LOS ALAMOS NATIONAL LABORATORY
ATTN: TECHNICAL STAFF (PLS ROUTE)
PO BOX 1663, MS D460
LOS ALAMOS, NM 87545

GARY MCCARTOR
SOUTHERN METHODIST UNIVERSITY
DEPARTMENT OF PHYSICS
DALLAS, TX 75275-0395

BRIAN MITCHELL
DEPARTMENT OF EARTH & ATMOSPHERIC SCIENCES
ST. LOUIS UNIVERSITY
3507 LACLEDE AVENUE
ST. LOUIS, MO 63103

JOHN MURPHY
MAXWELL TECHNOLOGIES
11800 SUNRISE VALLEY DRIVE SUITE 1212
RESTON, VA 22091

JAMES NI
NEW MEXICO STATE UNIVERSITY
DEPARTMENT OF PHYSICS
LAS CRUCES, NM 88003

PACIFIC NORTHWEST NATIONAL LABORATORY
ATTN: TECHNICAL STAFF (PLS ROUTE)
PO BOX 999, MS K6-48
RICHLAND, WA 99352

PACIFIC NORTHWEST NATIONAL LABORATORY
ATTN: TECHNICAL STAFF (PLS ROUTE)
PO BOX 999, MS K6-84
RICHLAND, WA 99352

ANATOLI L. LEVSHIN
DEPARTMENT OF PHYSICS
UNIVERSITY OF COLORADO
CAMPUS BOX 390
BOULDER, CO 80309-0309

DONALD A. LINGER
DNA
6801 TELEGRAPH ROAD
ALEXANDRIA, VA 22310

LOS ALAMOS NATIONAL LABORATORY
ATTN: TECHNICAL STAFF (PLS ROUTE)
PO BOX 1663, MS F665
LOS ALAMOS, NM 87545

LOS ALAMOS NATIONAL LABORATORY
ATTN: TECHNICAL STAFF (PLS ROUTE)
PO BOX 1663, MS C335
LOS ALAMOS, NM 87545

KEITH MCLAUGHLIN
MAXWELL TECHNOLOGIES
8888 BALBOA AVE.
SAN DIEGO, CA 92123-1506

RICHARD MORROW
USACDA/IVI
320 21ST STREET, N.W.
WASHINGTON, DC 20451

ROBERT NORTH
CENTER FOR MONITORING RESEARCH
1300 N. 17th STREET, SUITE 1450
ARLINGTON, VA 22209

JOHN ORCUTT
INSTITUTE OF GEOPHYSICS AND PLANETARY PHYSICS
UNIVERSITY OF CALIFORNIA, SAN DIEGO
LA JOLLA, CA 92093

PACIFIC NORTHWEST NATIONAL LABORATORY
ATTN: TECHNICAL STAFF (PLS ROUTE)
PO BOX 999, MS K6-40
RICHLAND, WA 99352

PACIFIC NORTHWEST NATIONAL LABORATORY
ATTN: TECHNICAL STAFF (PLS ROUTE)
PO BOX 999, MS K5-12
RICHLAND, WA 99352

FRANK PILOTTE
HQ/AFTAC/TT
1030 S. HIGHWAY A1A
PATRICK AFB, FL 32925-3002

JAY PULLI
BBN
1300 NORTH 17TH STREET
ROSSLYN, VA 22209

DAVID RUSSELL
HQ AFTAC/TTR
1030 SOUTH HIGHWAY A1A
PATRICK AFB, FL 32925-3002

SANDIA NATIONAL LABORATORY
ATTN: TECHNICAL STAFF (PLS ROUTE)
DEPT. 5704
MS 0979, PO BOX 5800
ALBUQUERQUE, NM 87185-0979

SANDIA NATIONAL LABORATORY
ATTN: TECHNICAL STAFF (PLS ROUTE)
DEPT. 5704
MS 0655, PO BOX 5800
ALBUQUERQUE, NM 87185-0655

THOMAS SERENO JR.
SCIENCE APPLICATIONS INTERNATIONAL CORPORATION
10260 CAMPUS POINT DRIVE
SAN DIEGO, CA 92121

ROBERT SHUMWAY
410 MRAK HALL
DIVISION OF STATISTICS
UNIVERSITY OF CALIFORNIA
DAVIS, CA 95616-8671

DAVID SIMPSON
IRIS
1200 NEW YORK AVE., NW
SUITE 800
WASHINGTON, DC 20005

BRIAN SULLIVAN
BOSTON COLLEGE
INSITUTE FOR SPACE RESEARCH
140 COMMONWEALTH AVENUE
CHESTNUT HILL, MA 02167

NAFI TOKSOZ
EARTH RESOURCES LABORATORY, M.I.T.
42 CARLTON STREET, E34-440
CAMBRIDGE, MA 02142

KEITH PRIESTLEY
DEPARTMENT OF EARTH SCIENCES
UNIVERSITY OF CAMBRIDGE
MADINGLEY RISE, MADINGLEY ROAD
CAMBRIDGE, CB3 OEZ UK

PAUL RICHARDS
COLUMBIA UNIVERSITY
LAMONT-DOHERTY EARTH OBSERVATORY
PALISADES, NY 10964

CHANDAN SAIKIA
WOOODWARD-CLYDE FEDERAL SERVICES
566 EL DORADO ST., SUITE 100
PASADENA, CA 91101-2560

SANDIA NATIONAL LABORATORY
ATTN: TECHNICAL STAFF (PLS ROUTE)
DEPT. 9311
MS 1159, PO BOX 5800
ALBUQUERQUE, NM 87185-1159

SANDIA NATIONAL LABORATORY
ATTN: TECHNICAL STAFF (PLS ROUTE)
DEPT. 5736
MS 0655, PO BOX 5800
ALBUQUERQUE, NM 87185-0655

AVI SHAPIRA
SEISMOLOGY DIVISION
THE INSTITUTE FOR PETROLEUM RESEARCH AND GEOPHYSICS
P.O.B. 2286, NOLON 58122 ISRAEL

MATTHEW SIBOL
ENSCO, INC.
445 PINEDA COURT
MELBOURNE, FL 32940

JEFFRY STEVENS
MAXWELL TECHNOLOGIES
8888 BALBOA AVE.
SAN DIEGO, CA 92123-1506

DAVID THOMAS
ISEE
29100 AURORA ROAD
CLEVELAND, OH 44139

LAWRENCE TURNBULL
ACIS
DCI/ACIS
WASHINGTON, DC 20505

GREG VAN DER VINK
IRIS
1200 NEW YORK AVE., NW
SUITE 800
WASHINGTON, DC 20005

TERRY WALLACE
UNIVERSITY OF ARIZONA
DEPARTMENT OF GEOSCIENCES
BUILDING #77
TUCSON, AZ 85721

JAMES WHITCOMB
NSF
NSF/ISC OPERATIONS/EAR-785
4201 WILSON BLVD., ROOM785
ARLINGTON, VA 22230

JIAKANG XIE
COLUMBIA UNIVERSITY
LAMONT DOHERTY EARTH OBSERVATORY
ROUTE 9W
PALISADES, NY 10964

OFFICE OF THE SECRETARY OF DEFENSE
DDR&E
WASHINGTON, DC 20330

TACTEC
BATTELLE MEMORIAL INSTITUTE
505 KING AVENUE
COLUMBUS, OH 43201 (FINAL REPORT)

PHILLIPS LABORATORY
ATTN: RESEARCH LIBRARY/TL
5 WRIGHT STREET
HANSCOM AFB, MA 01731-3004

FRANK VERNON
UNIVERSITY OF CALIFORNIA, SAN DIEGO
SCRIPPS INSTITUTION OF OCEANOGRAPHY IGPP, 0225
9500 GILMAN DRIVE
LA JOLLA, CA 92093-0225

DANIEL WEILL
NSF
EAR-785
4201 WILSON BLVD., ROOM 785
ARLINGTON, VA 22230

RU SHAN WU
UNIVERSITY OF CALIFORNIA SANTA CRUZ
EARTH SCIENCES DEPT.
1156 HIGH STREET
SANTA CRUZ, CA 95064

JAMES E. ZOLLWEG
BOISE STATE UNIVERSITY
GEOSCIENCES DEPT.
1910 UNIVERSITY DRIVE
BOISE, ID 83725

DEFENSE TECHNICAL INFORMATION CENTER
8725 JOHN J. KINGMAN ROAD
FT BELVOIR, VA 22060-6218 (2 COPIES)

PHILLIPS LABORATORY
ATTN: GPBP
29 RANDOLPH ROAD
HANSCOM AFB, MA 01731-3010

PHILLIPS LABORATORY
ATTN: PL/SUL
3550 ABERDEEN AVE SE
KIRTLAND, NM 87117-5776 (2 COPIES)